Research Square

Preprints are preliminary reports that have not undergone peer review.
They should not be considered conclusive, used to inform clinical practice,
or referenced by the media as validated information.

Symbiodiniaceae shifts in the corals Acropora cf. solitaryensis and A. aff. divaricata at the climate-driven poleward margin

Nina Yasuda

27yasuda@g.ecc.u-tokyo.ac.jp

The University of Tokyo https://orcid.org/0000-0002-9416-7754

Akifumi Shimura

Masumi Kamata

Hiroki Taninaka

Kenji Takata

Takashi Nakamura

Institute of Science Tokyo https://orcid.org/0000-0002-2434-4532

Akira Iguchi

National Institute of Advanced Industrial Science and Technology

Takehisa Yamakita

https://orcid.org/0000-0002-5451-1231

Satoshi Nagai

National Research Institute of Fisheries Science https://orcid.org/0000-0001-7510-0063

Taisei Kikuchi

The University of Tokyo https://orcid.org/0000-0003-2759-9167

Shota Shimizu

Hideaki Yusasa

Yuko Kitano

Kodai Gibu

Hironobu Fukami

Article

Keywords: climate change, range shift, connectivity, genetic diversity

Posted Date: August 30th, 2026

DOI: https://doi.org/10.21203/rs.3.rs-10532594/v1

License: This work is licensed under a Creative Commons Attribution 4.0 International License.
Read Full License

Additional Declarations: There is **NO** Competing Interest.

Symbiodiniaceae shifts in the corals *Acropora* cf. *solitaryensis* and *A.* aff. *divaricata* at the climate-driven poleward margin

Akifumi Shimura[1**], Masumi Kamata[2**], Hiroki Taninaka[3], Kenji Takata[2], Takashi Nakamura[4], Akira Iguchi[5,6], Takehisa Yamakita[7], Satoshi Nagai[8], Taisei Kikuchi[9], Shota Shimizu[10], Hideaki Yusasa[11], Yuko F. Kitano[12], Kodai Gibu[2], Hironobu Fukami[1], Nina Yasuda[2*]

Running title: Northernmost Corals Harbor Distinct Symbiotic Partners

[1]Faculty of Agriculture, University of Miyazaki, 1-1 Gakuen Kibanadai-nishi, Miyazaki, Japan

[2]Graduate School of Agricultural and Life Sciences, The University of Tokyo, Yayoi 1-1-1, Bunkyo-ku, Tokyo 113-8657, Japan

[3]Department of Chemistry, Biology, and Marine Science, Faculty of Science, University of the Ryukyus, 1, Sembaru, Nakagami Gun Nishihara Cho, Okinawa Ken, Japan

[4]Institute of Science Tokyo, 2-12-1-W8-5, O-okayama, Meguro-ku, Tokyo 152-8552, Japan

[5]Integrated Research Center for Nature Positive Technology, National Institute of Advanced Industrial Science and Technology (AIST) Umezono 1-1-1, Tsukuba, Ibaraki 305-8560, Japan

[6]Geological Survey of Japan, National Institute of Advanced Industrial Science and Technology (AIST), Umezono 1-1-1, Tsukuba, Ibaraki 305-8560, Japan

[7]Agency for Marine-Earth Science and Technology, 2-15, Natsushima-cho, Yokosuka-city, Kanagawa, 237-0061, Japan.

[8]Japan Fisheries Research and Education Agency, Fisheries Technology Institute, Coastal and Inland Fisheries Ecosystems Division, 2-12-4 Fukuura, Kanazawa-ku, Yokohama, Kanagawa 236-8648, Japan

[9]Department of Integrated Biosciences, Graduate School of Frontier Sciences, The University of Tokyo, Kashiwa 277-8652, Japan

[10]Tateyama Station, Field Science Center, Tokyo University of Marine Science and Technology, 670 Banda, Tateyama, Chiba 294-0308, Japan

[11]Independent researcher, Hyogo 651-0056, Japan

[12]Japan Wildlife Research Center, 3-3-7, Kotobashi, Sumida-ku, Tokyo 130-8606, Japan

Keywords: climate change, range shift, connectivity, genetic diversity

*Correspondence: Nina Yasuda

Graduate School of Agricultural and Life Sciences, The University of Tokyo, Yayoi 1-1-1, Bunkyo-ku, Tokyo 113-8657, Japan

Phone: +81-3-5841-8920, E-mail: 27yasuda@g.ecc.u-tokyo.ac.jp

**Akifumi Shimura and Masumi Kamata contributed equally to this work.

Abstract

Several reef-building corals are now extending their ranges northward into temperate areas. To test whether these edge populations show reduced host diversity or novel host–symbiont combinations, we analyzed two expanding *Acropora* species (*A.* cf. *solitaryensis* and *A.* aff. *divaricata*). Population genomic structure was estimated with Multiplexed ISSR Genotyping by Sequencing (MIG-seq), while Symbiodiniaceae assemblages were profiled by ITS2 sequencing. Host SNP data revealed comparable genetic diversity and generally high connectivity, with moderate differentiation at Tateyama. In contrast, Symbiodiniaceae communities at the two northernmost localities differed from those in the temperate-core habitats in that C3-radiation containing C115d variant was absent, whereas C1-radiation profiles were detected instead. Site-level exploratory analyses suggested that lower coldest-month seawater temperature was associated with higher C1-radiation occurrence, whereas chlorophyll a and turbidity showed weaker secondary associations. This provides an important field documentation of a pronounced spatial differentiation in Symbiodiniaceae assemblages associated with two dominant coral species at the leading edge of climate-driven range expansion.

Introduction

Coral reef ecosystems harbor almost 25% of the ocean biodiversity, yet they are among the ecosystems most vulnerable to climate change; effective conservation is therefore crucial [1-2]. It is well known that elevated water temperature caused by climate change can result in breakdown of obligate symbiosis between host reef-building coral and the unicellular alga Symbiodiniaceae, resulting in mass coral bleaching [3]. If the environmental stresses persist, corals will die. Thus, accumulating knowledge on coral adaptation in response to environmental changes caused by climate change is of great importance for future conservation of coral reefs.

There are a variety of factors, including coral genetic response, Symbiodiniaceae composition, and associated microbes, that would contribute to the coral tolerance to thermal stress [4-5]. Among many factors, Symbiodiniaceae composition is one important key for coral adaptation to climate change. Recent studies have substantially revised Symbiodiniaceae taxonomy, and the family is currently divided into 15 genera [6]. Within *Cladocopium,* many species broadly sort into two ITS2 radiations sensu LaJeunesse & Thornhill (2011) [7]: a C1-radiation (e.g., *C. goreaui, C. proliferum*, *C. vulgare*) and a C3-radiation (e.g., *C. thermophilum*, *C. patulum*, *C. sodalis*). Other minor C-lineages (e.g., C21, C42, C59) also occur but are not considered part of either radiation.

Relationships between Symbiodiniaceae composition and thermal tolerance of host corals [8-10] have been well-studied, especially in tropical areas where coral bleaching frequently occurs. There are several examples that show thermal tolerance of host corals is primarily determined by Symbiodiniaceae composition and corals change the composition before and after thermal stress: it is well known that corals have more thermal tolerance when having *Durusdinium* spp. and replace *Cladocopium* spp. to *Durusdinium* spp., although the growth

rate of juvenile corals is almost twice when having *Cladocopium* spp. rather than *Durusdinium* spp. [8-9]. A finer-scale example involves changes in *Cladocopium* ITS2 radiation. Following a bleaching event, *Acropora tenuis* colonies replaced their original C2-radiation profile with either a *Durusdinium* spp. profile or a C1-radiation profile: both symbiont lineages are associated with greater thermal tolerance [10]. In addition to Symbiodiniaceae composition, the shorter generation time of Symbiodiniaceae than coral host can facilitate faster local adaptation of thermal tolerance of coral species [11]. These previous studies underlined the importance of examining Symbiodiniaceae composition of corals for local adaptation.

While high thermal-temperature tolerance of corals with respect to Symbiodiniaceae composition is critical in tropical and subtropical regions, understanding low-temperature thermal tolerance with respect to Symbiodiniaceae composition is also essential in the context of global climate change. Some threatened coral species are now moving poleward and expanding their distribution in temperate regions such as the Japanese coast [12-15], Florida [16], Mediterranean [17], and Eastern and Western Australian coasts [18]. Now the northernmost habitats of *Acropora* corals in the Northern Hemisphere are Tateyama (34°59'27"N, 139°49'4"E) and Tsushima (34°25'25"N, 129°16'0"E) in Japan where water temperature has risen by 1.36 degrees in the last 100 years according to the Japan Meteorological Agency. These facts emphasize that cold water tolerance of corals with respect to Symbiodiniaceae composition is important for understanding and predicting the acclimatization potential of reef-building corals, especially at the shifting northernmost frontiers of coral distribution due to climate change. Nevertheless, low-temperature resistance of corals in association with Symbiodiniaceae composition is much less studied than heat resistance. Silverstein et al. (2017) demonstrated that corals harboring the ITS2 type D1a (*Durusdinium trenchii*) are more resilient to heat and cold stress than colonies dominated by

104 the C3-radiation [19]. LaJeunesse et al. (2014) also reported that ITS2 type D15 displays
105 physiological adaptations to low-temperature environments [20]. In line with these findings,
106 community-level surveys reveal that Symbiodiniaceae assemblages differ markedly between
107 tropical and temperate corals [21]. Although previous studies have examined how
108 environmental differences affect coral–Symbiodiniaceae associations, comprehensive, large-
109 scale investigations that correlate environmental variables with Symbiodiniaceae composition
110 across broader geographic ranges and numerous samples remain relatively rare.

111 In addition to the composition of Symbiodiniaceae and thermal stress of corals, the study of
112 genetic connectivity and diversity of host corals in northern habitats is essential to assess the
113 potential persistence of coral populations in face of climate change. Previous studies have
114 reported contrasting patterns of genetic diversity in marginal coral populations: genetic
115 diversity was reduced toward the poleward range margin in *Acropora hyacinthus*, whereas
116 populations from the recent northern expansion of *Oculina patagonica* harbored greater
117 genetic diversity than core and westward-expansion populations [14, 22]. These studies
118 suggest that connectivity by the current regional system and/or ecological characteristics of
119 each coral species determine the genetic diversity of newly colonized habitats. The
120 accumulation of knowledge on the genetic diversity and connectivity of different coral
121 species, including the northernmost coral populations, which represent the leading edge of
122 northward range expansion and pioneering new habitats, is important to predict for marine
123 conservation in the face of global climate change. In summary, recently colonized marginal
124 populations may experience harsh environmental conditions, potentially resulting in lower
125 genetic diversity and/or limited connectivity: however, they may also develop unique
126 adaptive strategies—particularly involving symbiotic partnerships—to better cope with cold
127 environments [19-22].

The objectives of this study were twofold: (i) to investigate the genetic diversity and connectivity of coral host species that appear to be undergoing a northward range expansion under climate change, and (ii) to characterize the Symbiodiniaceae compositions of corals in both the northernmost habitats and other regions, and to compare these findings with relevant environmental metrics. Ultimately, our goal is to gain insight into how corals and their symbiotic algae may collectively shift or expand their distributions in response to ongoing climate change. Such knowledge will support the development of predictive models that incorporate not only abiotic factors but also the critical biotic interactions necessary for understanding—and accurately forecasting—how symbiotic organisms will respond to and thrive under future environmental conditions.

Results

Sequencing and genotyping using MIG-seq

In MIG-seq analysis of *A*. cf. *solitaryensis*, a total of 23,727,250 raw reads with an average of 201,078 reads per sample were obtained for the 118 samples and after filtering out the low-quality reads, 23,545,458 reads remained. We obtained 11,468,148 reads with an average of 97,187 reads per individual after two-step filtering (removal of adaptors and short reads). After mapping on the *A. digitifera* reference genome, we obtained a total of 1583 SNPs (all SNPs option, STACKS option: -r 0.7) with 545 single SNPs (one SNP was chosen from each locus, STACKS option: -r 0.9). Of 118 samples, missing data ranged from 5.6% to 41.1% with an average of 17.8%. Of 1583 SNPs, BayeScan analysis indicated 8 SNPs were outlier loci ($0.05 > \alpha$ value, higher F_{ST} values than other loci). In MIG-seq analysis of *A.* aff. *divaricata*, a total of 46,207,812 raw reads with an average of 226,508 reads per sample were obtained for the 204 samples and after filtering out the low-quality reads, 45,868,110 reads remained. We obtained 29,154,622 reads with an average of 142,914 reads per individual

after two-step filtering. After mapping onto the *A. digitifera* reference genome, we obtained a total of 2,648 SNPs (all SNPs option, STACKS option: -r 0.7) with 673 single SNPs (one SNP was chosen from each locus, STACKS option: -r 0.9). Of 204 samples, the missing data ranged from 4.0% to 47.4% with an average of 18.4%. Of 2,648 SNPs, BayeScan analysis indicated 2 SNPs were outlier loci (0.05 > q-value, higher F_{ST} values than other loci).

In the MIG-seq analysis for algal symbiont genetic composition in *A*. cf. *solitaryensis* and *A.* aff. *divaricata*, a total of 25,092,972 raw reads with an average of 302,325 reads per sample were obtained for the 83 samples and after filtering out the low-quality reads, 24,921,038 reads remained. We obtained 9,886, 082 reads with an average of 119, 109 reads per individual after two-step filtering. After mapping on the *Cladocopium* spp. reference genome, we obtained a total of 110 SNPs (one SNP was chosen from each locus, STACKS option: -r 0.5). The DAPC was performed after removing individuals with more than 80% missing genotypes across the 110 retained loci.

Genetic diversity and genetic connectivity between populations of host coral species

Initial all-SNP datasets yielded 1,583 and 2,648 SNPs for *A*. cf. *solitaryensis* and *A*. aff. *divaricata*, respectively. After removal of candidate outlier loci, 1,575 and 2,646 loci were retained for downstream population analyses. Observed *heterozygosities* (H_o) ranged from 0.070 to 0.085 for *A*. cf. *solitaryensis* and from 0.063 to 0.079 for *A.* aff. *divaricata*, respectively, whereas expected *heterozygosities* (H_e) ranged from 0.085 to 0.106 for *A*. cf. *solitaryensis* and from 0.074 to 0.103 for *A.* aff. *divaricata*, respectively (Supplementary Table 1). The species boundary between *A.* cf. *solitaryensis* and *A.* aff. *divaricata* was confirmed by STRUCTURE analysis based on 411 SNP loci shared by the two species (Supplementary Fig. 1), consistent with the previous study [23].

Global F_{ST} values were both significant, with values of 0.061 ($p < 0.001$) in *A*. cf. *solitaryensis* and 0.032 ($p < 0.001$) in *A.* aff. *divaricata*. Pairwise F_{ST} values and PCoA suggested that the Tateyama population was relatively distinct from the remaining populations in both *A*. cf. *solitaryensis* and *A.* aff. *divaricata* (Fig. 1; Supplementary Table 2). The average pairwise F_{ST} value between Tateyama and the other populations was the highest in both species, with an average value of 0.084 in *A.* aff. *divaricata* and 0.095 in *A*. cf. *solitaryensis* (Supplementary Table 2). Similarly, PCoA based on population genetic data indicated that the eastern northernmost population, Tateyama was distinct from the remaining populations along PC1 in *A.* aff. *divaricata* and along PC2 in *A*. cf. *solitaryensis* (Fig. 1). However, another northernmost population, Tsushima, was not distinct from the remaining populations in either species. By contrast, STRUCTURE HARVESTER indicated $\Delta K = 2$ as the optimal number of clusters. At $K = 2$, STRUCTURE analysis of both species indicated genetic homogeneity across different sites including Tateyama in both coral species (Fig. 2). IBD was not significant in either *A*. cf. *solitaryensis* ($p = 0.120$) and *A.* aff. *divaricata* ($p = 0.160$) (Supplementary Fig. 2).

DAPC based on genome-wide SNP data from algal symbionts

DAPC based on 110 SNP loci identified six genetic clusters as the Bayesian information-criterion (BIC) optimum. We repeated the DAPC with both $K = 2$ (from STRUCTURE) and $K = 6$ (from the BIC curve). Under either assumption, the northernmost populations—Tateyama (TYA) and Tsushima (TUS)—of both *A.* cf. *solitaryensis* and *A.* aff. *divaricata* formed a distinct cluster from the more southerly populations, confirming their genetic separation from more southerly temperate populations (Fig. 3).

Haplotype network analysis of algae symbiont

After removing duplicated sequences obtained from the same coral colony, we obtained a total of 167 sequences (78 from *A.* cf. *solitaryensis* and 89 from *A.* aff. *divaricata*) from adult corals and 28 BLAST hit sequences in total from the juvenile samples (25 from *A.* cf. *solitaryensis* and 3 from *A.* aff. *divaricata*) (Supplementary Table 3). Blast search revealed all BLAST hit sequences obtained from adult corals were *Cladocopium* spp., whereas five *Symbiodinium* spp. (A-type) and its related haplotypes were found from juvenile corals in addition to *Cladocopium* spp. (Supplementary Table 4). Although juvenile corals are known to host greater diversity than adults [24], they contained C1-radiation haplotypes and lacked C115d clones. This pattern mirrors that of adults in the northernmost populations, except for the additional presence of Symbiodinium ITS2 type A haplotypes.

Note on terminology: Hereafter, C115d detected by SymPortal is referred to as DIV C115d within the C3-radiation, whereas C115d sequences obtained from subcloning are referred to as C115d clones. Additionally, ITS2 types such as C1 and C3 detected by subcloning are referred to as C1-radiation or C3-radiation haplotypes, while those detected by SymPortal are referred to as C1-radiation profiles or C3-radiation profiles to distinguish the analytical framework.

The haplotype network analysis constructed using *Cladocopium* sequences only, also showed the corals in two northernmost marginal populations (Tateyama and Tsushima) had distinct symbiont compositions in both species (Fig. 4). Both *A*. cf. *solitaryensis* and *A.* aff. *divaricata* hosted C1-radiation haplotypes. The only non-*Cladocopium* sequences were the five clade-A / *Symbiodinium* A-type sequences detected in *A*. cf. *solitaryensis* juveniles at Tateyama, which were excluded from the network and listed separately in Supplementary Table 4. By contrast, corals at all other sites were dominated by the C115d clones (Fig. 4).

At the two northernmost sites, we detected several previously unreported C1-radiation haplotypes, all of which were found exclusively in *A*. cf. *solitaryensis* (Fig. 4). Colonies of *A.* aff. *divaricata* at the same localities also hosted C1-radiation haplotypes, but no host-associated C1 haplotypes were observed in this dataset. Conversely, most C115d host-associated clones occurred in *A*. aff. *divaricata*, and almost no species-specific C115d clones were detected in *A*. cf. *solitaryensis.* We recovered 249 symbiont sequences from Tateyama seawater and 251 sequences from Miyazaki seawater by subcloning and BLAST analysis. Tateyama seawater yielded four C115d clones (1.61%) but no C1-radiation haplotypes, whereas Miyazaki seawater yielded 149 C115d clones, 11 C3-radiation haplotypes excluding C115d (in total 63.7%) and likewise no C1-radiation haplotypes (Supplementary Table 5). C1-radiation profiles were, however, detected by metabarcoding in Tateyama seawater collected in 2025 (Fig. 5; Supplementary Data 1-2).

Metabarcoding analysis of Symbiodiniaceae ITS2 amplicons using SymPortal

SymPortal ITS2 metabarcoding produced lineage patterns that were concordant with both the ITS2 haplotype network derived from subcloned sequences and the genome-wide population structure inferred from MIG-seq SNPs. Sequence quality metrics (read counts, no gap, N50, Q20, Q30, GC%) were satisfactory for both primer sets (Supplementary Data 3-4).

In all temperate populations except the two northernmost sites, the C3-radiation profiles including profiles containing DIV C115d, dominated the symbiont assemblages of both *A*. cf. *solitaryensis* and *A.* aff. *divaricata* (Fig. 5; Supplementary Fig. 3; Supplementary Data 1-2 and 5-6). By contrast, colonies from Tateyama and Tsushima—the range margin— were characterized by C1-radiation profiles together with low-abundance C3-radiation profiles and sporadic A-type signals. DIV C115d within the C3-radiation was absent from the two northernmost sites. (Fig. 5; Supplementary Fig. 3; Supplementary Data 1-2 and 5-6).

SymPortal ITS2 metabarcoding also revealed subtle differences between the two northernmost sites, Tsushima (TUS) and Tateyama (TYA): The Tsushima libraries were overwhelmingly composed of the C1-radiation profiles, whereas Tateyama retained appreciable proportions of C3-radiation variants (Fig. 5). At Tateyama, we also detected transient Symbiodinium (A-type) signals at low abundance in subadults (~10 cm) (Fig. 5; Supplementary Data 1-2).

Based on the SymPortal results for environmental samples, both C1-radiation and C3-radiation profiles were detected in seawater from Nishidomari, whereas only C3-radiation profiles, including profiles containing the DIV C115d, were detected in the Nobeoka seawater samples analyzed here (Fig. 5; Supplementary Data 1-2). Tateyama seawater contained both C1-radiation and C3-radiation profiles, but profiles containing the DIV C115d were not detected. In sediment samples, both C1-radiation and C3-radiation profiles, including profiles containing the DIV C115d, were detected at Nishidomari and Nobeoka, whereas Tateyama sediment was dominated by *Fugacium* and other minor profiles. Because environmental samples were collected in different years and seasons among localities, non-detection in a given environmental dataset should not be interpreted as definitive absence from that habitat.

Larval dispersal connectivity based on oceanographic model

Betweenness centrality calculated based on the oceanographic larval dispersal model showed a relatively low value in Tateyama (0.0016) compared to other sites, suggesting relative isolation of Tateyama from the rest of the coral habitats (Supplementary Table 6).

Environmental factors and C1- and C3-radiation profile occurrence

Because environmental predictors were defined at the site level, the GLMM results should be interpreted as exploratory site-level associations rather than as independent colony-level effects. The GLMM results were summarized in Supplementary Data 7 and 8. For C3-radiation profiles, among the GLMM results with single-variable models, the occurrence rate of the C3-radiation profiles showed a positive association with the mean seawater temperature of the coldest month (AIC = 40.30, AICc = 40.55). In this model, the mean seawater temperature of the coldest month had a positive coefficient (β = 2.85, S.E. = 1.47) with marginal statistical support (95% CI : -0.03 to 5.74, p = 0.053), suggesting potential positive association between higher water temperature and C3-radiation profile occurrence. While the model with the lowest AIC overall included temperature and chlorophyll a (AIC =38.50, AICc = 38.83), this model showed extremely large standard errors and non-informative estimates, including instability and poor parameter identifiability. Similarly, the full model failed to converge. Other environmental variables, including chlorophyll a and turbidity, showed no significant effects across all models (all $p > 0.1$), and their confidence intervals consistently overlapped zero. Taken together, these results suggest that the mean seawater temperature of the coldest month may weakly influence the C3-radiation profile occurrence, although this effect is not robust across model structures.

For the C1-radiation profiles, the best-supported model included the mean seawater temperature of the coldest month, average chlorophyll a, and turbidity (AIC = 60.00, AICc = 60.56). In this model, the mean seawater temperature of the coldest month had a negative effect on the occurrence of the C1-radiation profiles ($\beta = -9.77$, 95% CI = −14.60 to −4.94, $p < 0.001$), whereas both chlorophyll a and turbidity had much weaker but significant positive effects ($\beta = +1.45$, 95% CI = +0.59 to +2.31, $p < 0.001$; $\beta = +3.49$, 95% CI = +0.80 to +6.17, $p = 0.01$, respectively; Fig. 6). These results indicate that C1-radiation profiles were more likely to occur at sites with lower mean seawater temperature of the coldest month and higher

chlorophyll a concentration and turbidity. Models including the mean seawater temperature of the coldest month together with either chlorophyll-a alone or turbidity alone yielded qualitatively similar results, although with slightly weaker support (Supplementary Data 8). No overdispersion was detected in the best-supported model (dispersion ratio = 1.04, p = 0.89), and the site-level random effect was estimated to be negligible. In the null model, neither coral species nor primer set had a significant effect on C1-radiation occurrence. Because environmental predictors were defined at the site level, these results should be interpreted as site-level associations rather than independent colony-level effects.

Discussion

Corals changed their algal symbiotic partners at the forefront of the northward migration associated with climate change

Global climate change is now forcing a shift in the distribution of many marine species [25]. Range shifts of keystone species such as reef-building corals have cascading effects on biodiversity and the coastal environment, so it is critical to understand how such species adapt to high-latitude environments at the forefront of range shifts. The genetic composition of Symbiodiniaceae algae is recognized as a crucial determinant in the adaptation and survival of host corals. While most research has concentrated on heat tolerance, relatively few studies have addressed cold tolerance within the context of climate change [26-27]. This study provides the important field evidence that two dominant *Acropora* coral species exhibit a pronounced spatial shift in the composition of their symbiotic algae in cold environments at the leading edge of their climate change-driven range expansion.

The ITS2 haplotype network, metabarcoding analysis of Symbiodiniaceae ITS2 amplicons using SymPortal, and the DAPC based on genome-wide SNPs data all indicated that the Symbiodiniaceae compositions of the two *Acropora* spp. in the northernmost marginal

habitats (Tateyama and Tsushima) are different from the rest of the non-marginal populations. Interestingly, both *A.* cf. *solitaryensis* and *A.* aff. *divaricata* exhibited similar patterns of Symbiodiniaceae assemblages. At the northernmost sites, adult colonies were dominated by C1-radiation profiles, whereas C3-radiation profiles containing DIV C115d were not detected in host colonies. At Tateyama, C1-radiation and C3-radiation profiles were detected in seawater, but C3-radiation profiles containing the DIV C115d were not detected by SymPortal analysis. A small number of C115d clones were nevertheless recovered from Tateyama seawater by subcloning, indicating that C115d-containing C3-radiation sequences were present in the Tateyama environment. At the temperate-core localities Nishidomari and Nobeoka, environmental metabarcoding detected C1-radiation profiles at least in sediment samples, together with C3-radiation profiles including those containing DIV C115d. In seawater, both C1- and C3-radiation profiles were detected at Nishidomari, whereas only C3-radiation profiles, including DIV C115d-containing profiles, were detected at Nobeoka in the present dataset. The absence of C1-radiation profiles from Nobeoka seawater may reflect among-sample variation and limited sampling rather than true absence from the local environment. Thus, the present environmental data indicate that C1-radiation profiles can be locally available at temperate-core sites, although these environmental samples were not contemporaneous with host settlement and should be interpreted as qualitative snapshots. In the adult colonies examined from temperate-core localities, C1-radiation profiles were not detected within host colonies, whereas C3-radiation profiles containing DIV C115d predominated; however, species coverage and sample size were limited for Nobeoka. Together, these patterns suggest that environmental availability alone does not determine adult host symbiont composition. Because *Acropora* corals acquire symbionts horizontally [24, 28-29], partner selection likely occurs during the larval stage or soon after settlement. At Tateyama, juvenile colonies already contained C1-radiation haplotypes, whereas C115d

clones were absent (Fig. 4). The early presence of C1-radiation haplotypes and the consistent absence of C115d clones suggest preferential establishment or retention of C1-radiation haplotypes during early post-settlement development, and limited establishment of C115d clones. It is unlikely that the differences in host coral genotypes alone explain this shift in Symbiodiniaceae composition, as shown by overall genetic similarity across habitats in STRUCTURE analysis (Fig. 2). Even though Tateyama populations are somewhat isolated and differentiated from the rest of the populations as evidenced by centrality based on larval dispersal (Supplementary Table 6), overall genetic similarity was found between another northernmost population (Tsushima) and other populations (Fig. 1; Supplementary Table 1). Taken together, these patterns suggest that coral–symbiont associations across this latitudinal gradient are shaped by both host selectivity and local environmental availability, rather than by passive mirroring of the ambient symbiont pool alone: at the poleward limit, coral colonies establish symbiosis with C1-radiation profiles, whereas at the temperate-core sites, colonies preferentially harbor C3-radiation profiles dominated by the DIV C115d when DIV C115d-containing profiles are available in the environmental pool. Such uptake implies that host–symbiont specificity, together with availability plays a decisive role in structuring holobiont assemblages across this latitudinal gradient. The finding that only the northernmost populations had distinct symbiotic algal assemblages supports the hypothesis that the range-edge regions can promote sites of novel symbioses [30]. Previous studies have also reported that other coral species host C1-radiation profiles in high latitude and/or cold habitats such as Japan, South Korea, and Hong Kong [31-33]. However, caution is warranted in generalizing the association of C1-radiation profiles with cold water tolerance across all coral species, as algal symbionts can have opposite effects on different coral species [34]. GLMM results indicate that temperature was the strongest predictor of C1-radiation occurrence, with turbidity contributing secondarily to model fit. Associations with chlorophyll a were weaker

366 and model-dependent. These patterns raise the possibility that coral range expansion may be
367 influenced not only by host physiology but also by the local availability of suitable
368 Symbiodiniaceae lineages. Testing this idea will require physiological and ecological
369 analyses of atypical host–symbiont pairings.

370 Recent revisions to Symbiodiniaceae taxonomy have clarified that many widely used
371 *Cladocopium* ITS2 types correspond either to described species or to ITS2 profile sets; part
372 of the apparent diversity reflects intragenomic variants rather than species-level differences.
373 For instance, the well-known ITS2 lineage "C1" is best treated as an ITS2 radiation (sensu
374 LaJeunesse & Thornhill) comprising multiple described *Cladocopium* species (e.g., *C.*
375 *goreaui*, *C. proliferum*, *C. vulgare*) [7]. Consequently, records of the C1-type ITS2 profiles
376 should not be interpreted as a single symbiont species but rather as a set of closely related
377 lineages/species within the C1-radiation. The physiological differences among these closely
378 related taxa—and their contributions to coral thermal tolerance—remain only partially
379 resolved. Notably, despite the environmental availability of C1-radiation profile at temperate
380 core sites, neither coral sample in this study incorporated this symbiont, suggesting
381 environmental availability alone does not explain adult host symbiont composition.
382 Nonetheless, our data suggest that lineages within the *Cladocopium* C1-radiation may support
383 coral persistence in cold, range-edge environments, thereby helping to set the poleward limits
384 of coral distribution. Previous studies have also shown that different *Cladocopium* species
385 exhibit different physiological traits in corals: for example, colonies dominated by ITS2
386 profiles historically referred to as "C2-type" (not the clam-associated *C. infistulum*) have
387 been reported as more light-demanding and less thermotolerant than C1-type in *Acropora*
388 spp. on the Great Barrier Reef [10, 35]. While the previous studies have mostly investigated
389 the environmental tolerance of corals in relation to different genera (clades) of algal
390 Symbiodiniaceae, our research highlights that different algal symbiont lineages or ITS2

391 profile classes within the same genus can significantly influence coral resilience to low-
392 temperature stress.

393 Our results also show that the composition of coral symbionts undergoes a pronounced
394 spatial shift. Among the environmental variables included in our models, the mean seawater
395 temperature of the coldest month emerged as a weak predictor of C3-radiation profile
396 occurrence (Supplementary Data 7). In contrast, C1-radiation profiles were most closely
397 associated with lower temperature metrics (the mean seawater temperature of the coldest
398 month) and, to a lesser degree, higher turbidity (Fig. 6; Supplementary Data 8). Taken
399 together, these results suggest that temperature is the principal site-level correlate of C1-
400 radiation occurrence, whereas chlorophyll a and turbidity show weaker secondary positive
401 associations in the best-supported model.

402 **Conservation implications from genetic diversity and connectivity**

403 Contrary to *A. hyacinthus*, which has lower genetic diversity in recently colonized marginal
404 populations [14], the comparable heterozygosity across different regions suggests that genetic
405 diversity in the northernmost marginal populations of *A.* aff. *divaricata* is not significantly
406 lower than in other populations, although *A*. cf. *solitaryensis* in Tsushima has slightly lower
407 genetic diversity than other populations (Supplementary Table 1). The comparable neutral
408 genetic diversity in the recently colonized populations, including the northernmost site, to
409 other sites implies gene flow among these populations, consistent with the insignificant IBD
410 patterns (Fig 2; Supplementary Fig. 2). This comparable genetic diversity also suggests that
411 the marginal populations of the two *Acropora* species are not at higher risk of extinction and
412 are maintaining their evolutionary potential in terms of neutral genetic diversity, although
413 extinction risk cannot be concluded from neutral diversity alone. Given that the level of
414 neutral genetic diversity in marginal coral populations is species-specific, it is crucial to

assess the genetic diversity of each species including marginal habitats for effective conservation planning. In addition, assessing functional genetic diversity—particularly genomic regions associated with environmental tolerance—would greatly assist in predicting population persistence.

Given that the long-term conservation of species depends on genetically isolated populations with the potential for future speciation events [36], it is necessary to reconsider the value of the northernmost coral populations, particularly those at Tateyama. Tateyama populations are relatively isolated both physically and genetically from the other populations and may have potential for diversification including speciation. To effectively conserve these unique populations, it is critical to monitor the northward migration and local expansion patterns over time and determine whether these populations can serve as refugia for the species in the face of climate change.

Predicting the range limits of foundation species, such as corals, is crucial for conserving coastal ecosystems in the face of climate change [25]. Our field data suggest that corals in the northernmost habitats have recently undergone a pronounced spatial shift in their symbiont composition, potentially altering their environmental tolerance. Consequently, relying solely on the performance of corals from a single location to model species distributions may underestimate the importance of potential holobiont reorganization in novel environments or at range margins.

Traditionally, the northern limit of corals was thought to be determined primarily by the host's ability to withstand winter sea temperatures [37–38]. However, our findings indicate that the marked change in algal symbiont composition at the northern limit may also play a critical role in defining these boundaries. In particular, the environmental tolerance of symbionts—such as their capacity to thrive at lower temperatures—could be just as important

as host physiology in determining how far corals can extend. Further research should investigate whether the density and availability of these temperature-tolerant symbionts define the northernmost limits of coral habitats.

Methods

Study sites, target coral species and sampling and DNA extraction

In this study, genetic diversity and connectivity of two dominant temperate zone species (*A.* cf. *solitaryensis* and *A.* aff. *divaricata*) and their Symbiodiniaceae compositions in each habitat have been assessed**.**

Among coral species that are expanding their distribution in the last 90 years [15], *A. solitaryensis* species complex are fundamental coral species in Japanese temperate areas covering up to more than 80% of coral areas together with *A. hyacinthus* [39] and expand the habitats [15, 40]. The *A. solitaryensis* species complex in temperate Japan includes arborescent table (AR), solid plate (PL) and intermediate (IM) morphotypes. Based on recent morphometric and multilocus phylogenetic analyses [42], we treated AR colonies, which were previously included in *A. solitaryensis* sensu lato, as *A.* aff. *divaricata* and PL colonies as *A.* cf. *solitaryensis* throughout this study. The name *A.* cf. *solitaryensis* is used here for colonies previously referred to as *A*. cf. *glauca*, following Chow et al. [42]. Intermediate morphotypes, when present, were assigned to either *A.* aff. *divaricata* or *A.* cf. *solitaryensis* only when their host MIG-seq genotypes clearly clustered with one of these two taxa; otherwise, they were excluded from downstream analyses.

The *A. solitaryensis* species complex is a hermaphroditic, broadcast-spawner species whose fertilization takes place in the water column. Approximately 50% of *A.* aff. *divaricata* larvae can survive and settle around 21 days in the laboratory [43]. Therefore, it is likely that these

462 coral species can disperse over relatively long distances and move northward. In fact, the
463 northernmost habitats of the two species are currently Tateyama (34°59'27.00"N, 139°
464 49'4.00"E) in the east and Tsushima (34°25'25.00"N, 129° 16'0.00"E) in the west.

465 *A*. cf. *solitaryensis* and *A*. aff. *divaricata* were collected between September 2009 to July and
466 February 2026 from 10 locations spanning the temperate Japanese coast including the two
467 most recently colonized populations: Tsushima (the northwestern most) and Tateyama (the
468 northeastern most) (Fig. 7; Table 1). Additional adult corals were collected at Tateyama in
469 2024 and at Nobeoka in 2026. In the 2018 survey, several colonies collected at Tateyama and
470 Tsushima were juvenile corals (≦ 5 cm of the longest diameter) (Table 1; Supplementary Fig.
471 4). Because species-level identification of such small colonies is unreliable in situ, we
472 confirmed their host identity with MIG-seq data. To determine whether the symbiont patterns
473 observed in juveniles also apply to reproductively mature colonies, we collected additional
474 adult corals at Tateyama in 2024, Nobeoka in 2026. These additional Nobeoka colonies were
475 used only for adult Symbiodiniaceae composition and were not included in host population
476 genomic analyses or GLMMs. We collected less than 3 cm fragments of coral colonies from
477 each site to minimize the damage to the coral colonies via SCUBA and preserved them in
478 99% ethanol. Sampling was conducted under a Tokyo Prefectural Government Permit (No.
479 28-11) and a Kochi Prefectural Government Permit (No. 530 and No. 824). At other sites,
480 collecting permits from the local government were not required; however, we obtained prior
481 consent from the relevant local fisheries cooperatives before conducting the diving surveys.

482 We extracted genomic DNA from the ethanol-preserved coral samples using a modified hot
483 alkaline solution method [44] followed by ethanol precipitation [14, 45] or QIAGEN blood
484 and Tissue kit following manufacture's protocol depending on sample condition. These DNA
485 samples were used for genetic diversity analyses of both the coral host and its symbiotic

algae, focusing on MIG-seq loci. In addition, we examined Symbiodiniaceae composition through subcloning and Sanger sequencing of the ITS2 region (PCR product insertion into a vector, bacterial transformation, and colony isolation), as well as via metabarcoding using SymPortal.

Sample collection from surrounding seawater and sediment

To compare environmental Symbiodiniaceae composition between temperate-core and recently colonized marginal habitats, we collected seawater and sediment samples at Miyazaki, Tateyama, Nobeoka, and Nishidomari in 2020, 2025 and 2026 (Table 1). In Miyazaki, seawater samples were collected from a depth of 5 m on 26 March, 2020. In Nobeoka, seawater and sediment samples were collected from a depth of 9.5 m on 6 February, 2026. Additionally, in Nishidomari, we collected seawater and sediment samples around *A.* cf. *solitaryensis* or *A.* aff. *divaricata* on 30 January, 2026. In Tateyama, seawater samples were collected from a depth of 5 m on 31 October in 2020 and additional seawater and sediment samples were collected from a depth of 5 m on 21 February in 2025. Environmental samples were collected in different years and seasons among localities; these comparisons should therefore be interpreted as qualitative rather than strictly contemporaneous.

We used an MF-Millipore filter paper (Mixed cellulose esters membrane filter 0.45 μm AAWP) to filter up to 1L of seawater sample each in 2020. Genomic DNA was then extracted from three replicates of filter paper and subjected to DNA extraction. In 2025 and 2026, we used 0.22 or 0.45 μm Sterivex filter units (Millipore) for seawater samples. For each filter unit, up to 1 L of seawater was processed. The filter was then preserved in 1-2 mL of Qiagen ATL buffer or RNA later. Sediment samples were collected directly from the

seafloor using 50 ml of conical tubes and preserved in 99% ethanol or ATL buffer of QIAGEN DNeasy kit (Qiagen, Hilden, Germany).

For seawater samples collected in 2020 in Miyazaki and Tateyama, genomic DNA was extracted using Alkaline heating method from the filter [44].

For seawater samples collected in 2025 from Tateyama, and in 2026 from Nobeoka and Nishidomari, after bead-beating the samples, genomic DNA was subsequently extracted from both the ATL buffer and the filter membrane within the Sterivex unit using QIAGEN DNeasy kit (Qiagen, Hilden, Germany) based on protocol [46-47] and Qiagen PowerSoil kit (Qiagen, Hilden, Germany). A total of 7 replicate seawater samples from Tateyama, 5 samples from Nishidomari and 4 samples from Nobeoka were subjected to SymPortal analysis.

For sediment samples collected in 2025 from Tateyama, and in 2026 from Nishidomari and Nobeoka, after bead-beating the samples, genomic DNA was subsequently extracted from both the ATL buffer or ethanol preserved soil samples using the Qiagen PowerSoil kit (Qiagen, Hilden, Germany). A total of 6 replicates of Tateyama, 5 replicates of Nishidomari and 6 replicates of Nobeoka soil samples were subjected to SymPortal analysis.

MIG-seq analysis to obtain SNPs of host corals and algal symbiont

We performed a MIG-seq analysis, which amplifies neutral, anonymous genome-wide Inter-Simple Sequence Repeat (ISSR) regions. For this study, we performed multiplex ISSR PCR assays using MIG-seq primer set 2 (8 MIG-seq primer pairs) for the symbiotic algae and MIG-seq primer set 1 (16 MIG-seq primer pairs) for the host coral, respectively, following the protocol in [48] (Supplementary Table 7). Based on our preliminary experiments, the 16-primer set yielded a higher number of loci from the host coral genomes, whereas the 8-primer set was more effective in capturing Symbiodiniaceae SNPs. Consequently, we used the 16-

primer set for host coral analyses and the 8-primer set for Symbiodiniaceae. We used the Multiplex PCR Assay Kit Ver.2 (TaKaRa Bio Inc., Otsu, Shiga, Japan) for the first PCR. We mixed the 6 μL reagent and 1 μL template DNA, and then, the first PCR protocol was as follows: 1 min denaturation at 94 ℃ followed by 30 cycles of 30 s at 94 ℃, 1 min at 38 ℃, 1 min at 72 ℃, with a final 10 min extension at 72 ℃. The first PCR products were diluted 50 times to prepare the template for the second PCR. The second PCR was executed to add the individual index and the Illumina adapter sequence to each first PCR sample. We used primeSTAR GXL DNA polymerase (TaKaRa Bio Inc., Otsu, Shiga, Japan) for second PCR. We prepared a total volume of 12 μL reaction reagent and thermocycling parameters were as follows: 20 cycles at 98 °C for 10 s, 54°C for 15 s, 68 °C for 1 min. We mixed 1 μL of each second product as library and refined it. Next, we electrophoresed on 1% agarose gel to check amplification. We selected the size ranged from 350 to 800 bp, and then, the DNA of specific size was manually extracted from the gel on a transilluminator. We extracted genomic DNA from the gel using FastGene Gel/PCR Extraction Kit (Nippon Genetics, Tokyo, Japan). We used MiSeq (sequencing control software v2.0.12, Illumina) and the MiSeq Reagent v3 150 cycle kit (Illumina) to sequence the DNA libraries from each sample with a different index. For host coral population genomic analysis, we used all the samples we collected (118 *A.* cf. *solitaryensis* and 204 *A.* aff. *divaricata* individuals), geographically separated by up to 960 km (Table 1). As part of our quality control process, we used the FASTX-toolkit v. 0.0.14 (fastq_quality_filter) [49] with parameters Q = 33, q = 30, and p = 40 to remove low-quality reads and primer sequences. We then employed Cutadapt v. 1.13 [50] with the -e 0.05 option to trim Illumina MiSeq adapter sequences from both the 5′ end (GTCAGATCGGAAGAGCACACGTCTGAACTCCAGTCAC) and the 3′ end (CAGAGATCGGAAGAGCGTCGTGTAGGGAAAGAC). Finally, reads shorter than 80 bp were excluded. The quality-filtered sequence data were demultiplexed through the software

Stacks v2.2 [51-52]. We genotyped the reads with the gstacks module of STACKS v2.2 [51-52]. Reads were mapped to the *A. digitifera* reference genomes for host coral analyses [53] and to the symbC.v1.0 genome originally described as *Symbiodinium* sp. clade C [54] and now classified within *Cladocopium,* for Symbiodiniaceae analyses. GSTACKS reads all input files simultaneously from external alignment program BWA-MEM [55] (https://arxiv.org/abs/1303.3997) and scans the genome for MIG-seq loci using a sliding window method. We used the gstacks --rm-pcr-duplicates option to remove PCR duplicates by randomly retaining one read pair from each duplicate set. For the coral genetic analyses, we used the STACKS populations program. Depending on the analysis, loci present in at least 70 % or 90 % of individuals (-r 0.7 or -r 0.9) were retained. We set a minimum minor-allele frequency of 0.01 and a maximum observed heterozygosity of 0.99. To avoid linkage between loci, we used the -write-single-snps option to select only one SNP per locus. BayeScan v 2.0 [56] was used to detect possible SNPs under natural selection assuming different species or populations with a default setting for each data set. PGDspider v. 2.0.8.3 [57] was used for data file conversion whenever needed. All MIG-seq data of the coral and algal symbiont are deposited through DDBJ (322 datasets with 16-primer set: DRR638658-DRR638979 and 83 datasets with 8-primer set: DRR636256-DRR636339 excluding DRR636321). DRR636321 was excluded because the corresponding sample was suspected of contamination.

Genetic diversity and connectivity analysis of coral species

For genetic diversity indices, we calculated observed heterozygosities (H_O) and expected heterozygosities (H_E) for each population and species using GenAlEx v. 6.5 [58]. Pairwise F_{ST} values were also calculated to estimate genetic connectivity among populations within

each species using GenAlEx v. 6.5 [58]. To visualize genetic relationship among populations, Principal Coordinate Analysis (PCoA) was also conducted using GenAlEx v. 6.5 [58].

STRUCTURE v. 2.3.4 [59] was employed to perform a Bayesian individual-based assignment test, allowing us to infer population structure and assess admixture among different sampling sites. Here, "genetic admixture" refers to the historical or ongoing mixing of distinct ancestral lineages 10 independent runs were performed in STRUCTURE using an admixture model. We used an allele frequency correlated model with uniform prior. Both the length of the burn-in period and the number of Markov Chain Monte Carlo analyses (MCMC) were 500,000. We estimated ΔK [60]—the statistic used to determine the most likely number of clusters—by applying STRUCTURE HARVESTER [61]. Here, K represents the number of assumed ancestral population clusters, and each individual's genetic membership is probabilistically assigned across these clusters. CLUMPAK [62] was used to summarize and visualize the STRUCTURE results. STRUCTURE analyses were conducted using three different datasets: (i) *A.* cf. *solitaryensis* and *A.* aff. *divaricata* samples to confirm genomic species boundaries, (ii) *A.* cf. *solitaryensis* samples, and (iii) *A.* aff. *divaricata* samples.

To examine the isolation by distance patterns (IBD) of each coral species, pairwise genetic distances $F_{ST}/(1 - F_{ST})$ were regressed on linear geographic distances between populations. We performed Mantel tests as implemented in GenAlEx v. 6.5 [58].

Genetic compositions of Symbiodiniaceae based on MIG-seq loci

To examine Symbiodiniaceae population genomic patterns, we used the populations module of STACKS to extract loci that occurred in at least 50% of individuals in each dataset (-r 0.5) and to filter the minimum minor allele frequency required to process a nucleotide site at a locus of 0.01 and the maximum observed heterozygosity required to process a nucleotide site

at a locus of 0.99. To remove linkage between loci, we used the -write-single-snps option to select only one SNP per locus. Discriminant Analysis of Principal Components (DAPC) [63-65] was performed to visualize the genetic structure (adegenet package v. 2.1.10 in R v. 4.5.1), with all SNPs of 110 loci of 83 samples (DRR636256-DRR636339 excluding DRR636321), using 7 sites (Goto, Miyazaki, Tsushima, Yokonami, Wakayama, Shikinejima, Tateyama) where two coral species are collected sympatrically. We excluded 13 individuals with more than 80% missing genotypes across the 110 retained loci. The DAPC was performed on the remaining 70 individuals. The lowest BIC was used to detect the optimal number of *K* clusters.

ITS2 cloning and sequencing of symbiont compositions

We identified Symbiodiniaceae haplotypes by subcloning the ITS2 region and examined their evolutionary relationship. Using the subcloning method, PCR-amplified Symbiodiniaceae ITS2 fragments were inserted into plasmid vectors and introduced into Escherichia coli cells. Successful transformants containing the ITS2 insert were then identified by blue–white screening, thereby providing abundant ITS2 clones for further analysis. We used commonly used symbiont primers ITSintfor2 and ITS-Reverse [66-67] to amplify 287 bp of ITS2 region from the coral samples and the filtered seawater samples. Thermocycling parameters were as follows: 3 min denaturation at 94 ℃ followed by 35 cycles of 30 s at 94 ℃, 30 s at 52 ℃, 30 s at 72 ℃, with a final 5-min extension at 72 ℃. Each PCR mixture (10 μL) consisted of 5 μL of KAPATaq HS ReadyMix with dye (Nippon Genetics), 0.7 μL of each primer (50 μM), 3.86 μL of double-distilled water, and 1 μL of template DNA. pGEM-T (Easy) Vector Systems (Promega) was used for cloning following the manufacturer's protocol. We picked up 10 to 12 colonies per coral sample. Inserts in the colonies were reamplified by PCR using M13 and U19 primers. One microliter of PCR product was cleaned using ExoSap-IT

(Affymetrix) following manufacturer's protocol and then incubated at 37 ℃ for 15 min and 80 ℃ for 15 min. The cleaned PCR products were sequenced using U19 primer on an ABI 3130xl automated sequencer using BigDye ver. 3.1 terminator chemistry (Applied Biosystems, Foster City, CA). We manually checked sequencing errors using BioEdit v. 7.0.9.0 [68] and then aligned all the sequences using GENETIX v. 12 (https://www.genetyx.co.jp/products/genetyx_12/index.html). After BLAST search for each sequence, we excluded the duplicated haplotype sequences found in the same coral colony. The haplotype diversity of the symbiont for each population was estimated using DnaSP v. 5 [69]. A median-joining network [70] was constructed using NETWORK v. 10 with the default settings to visualize evolutionary relationships. We excluded 5 sequences of *Symbiodinium* spp. (A-type sequence, separtely listed in Supplementary Table 4) found in juveniles in the haplotype network analysis because they are genetically too divergent from *Cladocopium* spp. We submitted the sequence data of ITS2 through DDBJ (Accession number: LC889618-LC889976).

Metabarcoding analysis of Symbiodiniaceae ITS2 amplicons using SymPortal.

The ITS2 region of Symbiodiniaceae ribosomal DNA operon was targeted for sequencing using Symbiodiniaceae specific primers ITSintfor2 and ITS-Reverse [66-67], and SYM_VAR_5.8S2 and SYM_VAR_REV [71-72] (Supplementary Table 7). Sample details were summarized in Table 1. PCR amplification for 46 coral samples and seawater samples collected in 2020 was carried out using the ITSintfor2 and ITS-Reverse primers as described in [73]. Each 25 μL reaction contained 1.0 μL of template DNA, 2.5 μL of each dNTP, 1× PCR buffer, 2.5 μL of Mg^{2+}, 0.5 μL of KOD-Plus-Ver.2 (TOYOBO, featuring robust 3′ → 5′ exonuclease activity), and 1.0 μL (10 μM) of each primer [73]. The PCR cycling conditions were as follows: initial denaturation at 94 °C for 3 min: 30 cycles at 94 °C for 15

s, at 56 °C for 30 s and at 68 °C for 40 s. Results of PCR amplification were checked by agarose gel electrophoresis. PCR amplification was evaluated by 1% agarose gel electrophoresis. The PCR products were purified using an Agencourt AMPure XP (BECKMAN COULTER, Life Sciences, Brea, California, USA) according to the manufacturer's protocol. Index and adaptor sequences were attached during the second PCR step using the following primer set: 5'-AATGATACGGCGACCACCGAGATCTACAC- 8 bp index -ACACTCTTTCCCTACACGACGC (forward) and 5'-CAAGCA GAAGACGGCATACGAGAT- 8 bp index -GTGACTGGAGTTCAGACGTGTG (reverse). The 8 base segments represent dual-index sequences used to recognize each sample. The purified first-round PCR product was diluted 5 times with molecular grade water and used as a template for the second-round PCR. The second-round PCR was carried out with the same condition as the first-round PCR, except ten cycles of the PCR with the annealing temperature was 59 °C. The PCR products were purified using an Agencourt AMPure XP again and quantified to pooled in equal concentrations. We sequenced using the Illumina miSeq v.3 Reagent kit for 2× 300 bp PE.

We used the SYM_VAR_5.8S2 and SYM_VAR_REV primers [71-72] to analyze a total of 89 adult coral samples. This dataset comprises (i) adult colonies from the other locations that had been collected and analyzed before 2024 but were re-processed with the current pipeline, and (ii) additional adult colonies collected at Tateyama in 2024. All juvenile specimens were excluded. The first PCR was performed in a reaction mixture (10 µL) containing 1.0 µL- 3.0 µL of template DNA, 3.5 µL of dH_2O, 5.0 µL of KOD One PCR Master Mix or KOD One PCR Master Mix -Blue- (TOYOBO) and 0.5 µL (10 µM) of each primer. The PCR cycling conditions were as follows: hot start at 98 °C for 1 min, followed by 28 cycles of 98 °C for 10 sec, 56 °C-58 °C for 5 sec, and 68 °C for 5 sec, concluding with a final extension at 68 °C for 5 min. After PCR, the PCR products were held at 12 ℃ and stored at refrigerated

677 temperatures. The first PCR products were purified using an Agencourt AMPure XP
678 (Beckman Coulter, Brea, CA, USA) according to the manufacturer's protocol or automatic
679 protocol using KingFisher Apex System (Thermo Fisher). The purified first-round PCR
680 product was used at original condition or modified three times condition for template of the
681 second PCR to attach an overhang adaptor sequence amplifying the ITS2 rDNA region. Index
682 and adapter sequences were incorporated during the second PCR, and introduced Illumina-
683 compatible overhangs and dual 8 bp indices, enabling sample identification and library
684 preparation for SymPortal analysis. The second PCR was performed in a reaction mixture (20
685 μL) containing 1.0 μL of template DNA, 12.1 μL of dH_2O, 2.0 μL of 10 × buffer, 1.6 μL of
686 dNTP, 0.1 μL of EX Taq (TaKaRa Bio Inc., Otsu, Shiga, Japan) and 1.6 μL (5 pM) of each
687 primer. The PCR cycling conditions were as follows: hot start at 96 ℃ for 1 min, followed by
688 15 cycles of 96 ℃ for 30 sec, 65 ℃ for 45 sec, and 72 ℃ for 60 sec, concluding with a final
689 extension at 72 ℃ for 7 min. After PCR, the PCR products were stored at refrigerated
690 temperatures. The PCR products were purified using an Agencourt AMPure XP again and
691 quantified to pooled in equal concentrations. We sequenced using the Illumina MiSeq
692 Reagent Nano Kit v2 (500 Cycles) MS-103-1003 for 2× 250 bp PE. The first and second
693 PCR results were checked by agarose gel electrophoresis before proceeding with the next
694 step.

695 Obtained fastq files were processed with the SymPortal v. 0.3.15 [74]. The fastq files
696 obtained were deposited in the DNA Data Bank of Japan (DDBJ) (DRR699761-DRR699806,
697 DRR702774-DRR702888 and DRR918851-DRR918879). SymPortal is an analytical
698 framework for phylogenetically resolving putative taxa within the Symbiodiniaceae using
699 NGS data of the ITS2 amplicon. Sequencing data were analyzed by SymPortal using a
700 standardized approach across all analytical steps to ensure reproducibility and transferability

across studies [74]. In SymPortal, sequence quality control was performed using mothur, the BLAST + suite, and minimum entropy decomposition (MED) using default parameters. Sequence reads were screened for a minimum overlap of 30bp and sequences with ambiguous base calls were removed using mothur. The blastn program from the blast+ suite of executables was used to identify sequences such as Symbiodiniaceae or non-Symbiodiniaceae. Minimum Entropy Decomposition (MED) provides a computationally efficient means to partition marker gene datasets into 'MED nodes', which represent homogeneous operational taxonomic units [75]. MED nodes were determined by looking at each nucleotide position in the set of sequences and seeing which of these positions are most informative in differentiating between the sequences of the dataset. ITS2 amplicon reads were processed with the SymPortal analytical framework to infer Symbiodiniaceae ITS2 type profiles, defined as sets of recurrent, co-occurring defining intragenomic variants (DIVs) within a sample. Profiles were assigned to genera by DIV suffix (A, C, D, etc.). For downstream visualization and modelling, *Cladocopium* profiles were mapped to radiations by their core DIV—profiles containing C1 were treated as C1-radiation and those containing C3 (including the variant C115d) as C3-radiation—whereas A-type (*Symbiodinium*) profiles were retained separately. Samples with < 100 Symbiodiniaceae reads after quality filtering were excluded. All statistical analyses for metabarcoding were performed in R v. 4.5.1. For visualization, we collapsed the SymPortal ITS2 type profiles to the radiation level and used a gradient palette to highlight C1- and C3-radiation profiles in distinct color families. Profiles belonging to other *Cladocopium* radiations or to different genera (e.g., *Symbiodinium* [A-type], *Fugacium* [F-type]) are shown in genus-specific color families, each rendered as gradients to indicate within-genus variation. To visualize the data, we used R packages ggplot2 v 3.5.2 (https://cran.r-project.org/web/packages/ggplot2/index.html), reshape2 v 1.4.4

(https://cran.r-project.org/web/packages/reshape2/index.html) and dplyr v 1.1.4 (https://cran.r-project.org/web/packages/dplyr/index.html).

It is important to note that the "C1-radiation" category in our haplotype network and the "C1-radiation profile" ITS2 type profile in SymPortal are derived by different pipelines and different sample sets—our network retains every unique sequence potentially including PCR or sequencing artefact, whereas SymPortal collapses near-identical variants into a single profile—so the two classifications overlap but are not identical.

Note that seawater and sediment datasets were used in three distinct ways. First, the 2020 Miyazaki and Tateyama seawater samples were used for ITS2 subcloning and for the ITSintfor2/ITS-Reverse SymPortal dataset. Second, the 2025 Tateyama and 2026 Nishidomari/Nobeoka seawater and sediment samples were analyzed with the SYM_VAR primer set and are shown in Fig. 5. Third, only the adult coral SymPortal presence/absence matrix was used for the GLMMs; environmental seawater and sediment samples were used descriptively and were not included as response data in the GLMMs.

Environmental data

Climatological average chlorophyll a, turbidity, and sea surface water temperatures (annual average, monthly average minimum seawater temperature, and monthly average maximum seawater temperature) were obtained as environmental data for coral habitats from MODIS satellite data (NASA Ocean Biology Processing Group. (2017). MODIS Level-3 Ocean Color Data, NASA Ocean Biology Distributed Active Archive Center. Accessed on 2024/06/09). Centrality (betweenness, closeness) was calculated for each sampling location using the graph library in R based on the larval dispersal connectivity of particles previously calculated by [14]. In short, an average connectivity matrix was obtained by conducting the Lagrangian particle tracking simulation using Global HYCOM ocean-current data for a total of 24 years

from 1993 to 2016. We used the larval-dispersal simulation to calculate a centrality metric for each site, providing an index of habitat isolation. Spawning of *Acropora* was modelled to begin three days before the spawning full moon and to continue for ten days once the cumulative thermal anomaly—calculated as the integral of max (T-13 °C, 0) from 1 February—exceeded 1,000 °C·day. This "1,000 degree-day" threshold is an empirically derived value that best reproduces the observed timing of *Acropora* spawning throughout the study region [14].

Generalized Linear Mixed Model (GLMM) analysis of Symbiodiniaceae type composition versus environmental predictors

To investigate which environmental factors correlate with shifts in the Symbiodiniaceae composition of two northward-expanding coral species, we performed Generalized Linear Mixed Model (GLMM) analyses on presence–absence data for C1-radiation profile and C3-radiation profile. These data were obtained from 111 colonies (59 of AcS and 52 of AaD) through SymPortal analyses involving two primer sets (ITSintfor2/ITS-Reverse and SYM_VAR_5.8S2/SYM_VAR_REV). When both primer sets were available for the same colony, the colony was represented only once in the GLMM dataset after harmonizing radiation-level presence/absence calls. Because multiple coral colonies were sampled at each site whereas environmental covariates were defined at the site level, colonies from the same site were not statistically independent. To account for this within-site non-independence, all GLMMs included sampling location as a random intercept (1 | site). However, the model coefficients and *P* values should be interpreted as exploratory site-level associations, not as independent colony-level causal effects. Adult colonies collected at Tanegashima in 2018 and Nobeoka in 2026 were used descriptively for Symbiodiniaceae composition but were excluded from the GLMM dataset because they did not include both coral species, or had

small sample sizes, and lacked colony-level environmental matching data. After assessing multicollinearity by calculating variance inflation factors (VIFs), we used the mean seawater temperature of the coldest month, mean chlorophyll a concentration, and turbidity as explanatory variables, all of which were standardized by Z-score transformation. Therefore, our GLMMs either included only one environmental variable at a time or combined two or three non-collinear variables in the following ways: (i) average chlorophyll a plus turbidity, (ii) the mean seawater temperature of the coldest month plus average chlorophyll a, (iii) the mean seawater temperature of the coldest month plus turbidity, or (iv) the mean seawater temperature of the coldest month, average chlorophyll a, and turbidity. We fitted these models in R v. 4.5.1 using the glmmTMB package (v. 1.1.11: [76]) under a binomial distribution with a logit link function, incorporating sampling site information as a random effect. Model selection was based on AIC and AICc, and overdispersion was evaluated with the performance package (v. 0.15.0: [77]) and MuMIn (v. 1.48.19; https://cran.r-project.org/web/packages/MuMIn/index.html). Due to limited sample size, certain models failed to converge and were consequently excluded from further analysis. We used R packages ggplot2 v 3.5.2 (https://cran.r-project.org/web/packages/ggplot2/index.html), ggeffects v 2.3.0 (https://strengejacke.github.io/ggeffects/news/index.html) and tidyverse v 2.0.0 (https://cran.r-project.org/web/packages/tidyverse/index.html) to visualize the results of GLMM.

Statistics and reproducibility

All statistical analyses were conducted in R (v. 4.5.1) and GenAlEx v. 6.5. For Symbiodiniaceae metabarcoding, ITS2 reads were processed in SymPortal (v. 0.3.15) to infer ITS2 type profiles (sets of co-occurring DNA variable regions (DIVs)). For modelling purposes, the profiles were mapped to the radiation level (C1-radiation; C3-radiation

including C115d). Samples with fewer than 100 Symbiodiniaceae reads after quality control were excluded. The presence or absence of each radiation was analyzed using GLMMs (binomial, logit link; glmmTMB, n = 111) with Z-standardised environmental predictors. Multicollinearity was checked using VIF, and models were compared using AIC and AICc. Confidence intervals (95%) were estimated for GLMMs. Random intercept for sampling location was specified as detailed in the Methods section. Overdispersion diagnostics and full model outputs are provided in Supplementary Data 7-8. For host and algal MIG-seq analyses, the filtering thresholds for SNPs and program settings were set out in the Methods section. Summary diversity indices and ordinations were computed using standard packages (see figure legends and Supplementary Tables for details). We collected at least six samples of two coral species, *A.* aff. *divaricata* and *A.* cf. *solitaryensis*, from each area whenever possible for MIG-seq and metabarcoding analyses. In some areas, however, the number of samples was fewer than 6 due to low DNA concentrations and substantial sequence loss. For population genetic analyses, we used datasets comprising more than 10 samples. In addition, seawater and sediment samples were collected with at least four replicates from each site where coral habitats were present. Biological replicates were independent coral colonies without clonemates in all MIG-seq analyses and GLMMs. Environmental replicates comprised independent seawater filters (Tateyama: n = 7; Nishidomari: n = 5; Nobeoka: n = 4) and independent sediment grabs (Tateyama: n = 6; Nishidomari: n = 5; Nobeoka: n = 6). Juveniles were excluded from the GLMM dataset. Field collections were not randomized or blinded, but laboratory procedures were standardized and applied uniformly across sites and years. The exact model formulas, parameter settings and library size summaries can be found in the Supplementary Information, and the raw sequence data have been deposited under the DDBJ accessions listed in the Data Availability Statement.

Data Availability Statement

The raw sequencing data have been deposited in the DNA Data Bank of Japan (DDBJ) as follows: MIG-seq (host corals, 16 primer set): DRR638658–DRR638979 (https://ddbj.nig.ac.jp/search/entry/bioproject/PRJDB18296). MIG-seq (Symbiodiniaceae, 8-primer set): DRR636256–DRR636339 excluding DRR636321 (https://ddbj.nig.ac.jp/search/entry/bioproject/PRJDB18642). ITS2 metabarcoding (SymPortal runs; FASTQ): DRR699761-DRR699806, DRR702774-DRR702888 and DRR918851-DRR918879 (https://ddbj.nig.ac.jp/search/entry/bioproject/PRJDB20741; https://ddbj.nig.ac.jp/search/entry/bioproject/PRJDB20640; https://ddbj.nig.ac.jp/search/entry/bioproject/PRJDB40644). The processed datasets needed to reproduce the figures and statistics are provided in Supplementary Data 1-8: SymPortal ITS2 type-profile tables; per-sample read counts and library statistics (Supplementary Data 3-4); radiation-level presence/absence matrices used for GLMMs (Supplementary Data 1-2 and 5-6). Additionally, the raw ITS2 sequencing data have been deposited in DDBJ and are accessible via the DDBJ GetEntry system (https://getentry.ddbj.nig.ac.jp/top-j.html) under accession numbers LC889618–LC889976.

Environmental covariates (MODIS Level-3 chlorophyll a, turbidity and SST) are publicly available from NASA's Ocean Biology Data Archive (OBDAAC); the exact products and access dates are listed in the Methods section. The site-level centrality metrics derived from the larval dispersal model are provided in Supplementary Table 6.

Code Availability

The code used for MIG-seq analyses is available on Zenodo and GitHub. (https://doi.org/10.5281/zenodo.17431289, https://github.com/ninayasuda/old-MIGseq/blob/main/mig_mapping2.sh).

References

1. Wilkinson, C. R. Global and local threats to coral reef functioning and existence: review and predictions. *Mar. Freshwater Res.* **50**, 867–878; 10.1071/MF99121 (1999).

2. Hughes, T. P. *et al.* Climate change, human impacts, and the resilience of coral reefs. *Science* **301**, 929–933; 10.1126/science.1085046 (2003).

3. Brown, B. E. Coral bleaching: causes and consequences. *Coral Reefs* **16**, S129–S138; 10.1007/s003380050249 (1997).

4. Baums, I. B. *et al.* Genotypic variation influences reproductive success and thermal stress tolerance in the reef building coral, *Acropora palmata*. *Coral Reefs* **32**, 703–717; 10.1007/s00338-013-1012-6 (2013).

5. Cziesielski, M. J., Schmidt-Roach, S. & Aranda, M. The past, present, and future of coral heat stress studies. *Ecol. Evol.* **9**, 10055–10066; 10.1002/ece3.5576 (2019).

6. Nitschke, M. R. *et al.* The diversity and ecology of Symbiodiniaceae: A traits-based review. *Adv. Mar. Biol.* **92**, 55–127; 10.1016/bs.amb.2022.07.001 (2022).

7. LaJeunesse, T. C. & Thornhill, D. J. Improved resolution of reef-coral endosymbiont (Symbiodinium) species diversity, ecology and evolution through psbA non-coding region genotyping. *PLoS One* **6**, e29013; 10.1371/journal.pone.0029013 (2011).

8. Silverstein, R. N., Cunning, R. & Baker, A. C. Change in algal symbiont communities after bleaching, not prior heat exposure, increases heat tolerance of reef corals. *Glob. Change Biol.* **21**, 236–249; 10.1111/gcb.12706 (2015).

9. Mieog, J. C. *et al.* The roles and interactions of symbiont, host and environment in defining coral fitness. *PLoS One* **4**, e6364; 10.1371/journal.pone.0006364 (2009).

867 10. Jones, A. M. *et al.* A community change in the algal endosymbionts of a scleractinian
868 coral following a natural bleaching event: field evidence of acclimatization. *Proc. R. Soc. B*
869 **275**, 1359–1365; 10.1098/rspb.2008.0069 (2008).

870 11. Howells, E. J. *et al.* Coral thermal tolerance shaped by local adaptation of
871 photosymbionts. *Nat. Clim. Change* **2**, 116–120; 10.1038/nclimate1330 (2012).

872 12. Mezaki, T. & Kubota, S. Changes of hermatypic coral community in coastal sea area of
873 Kochi, high-latitude, Japan. *Aquabiology* **201**, 332–337 (2012).

874 13. Nakabayashi, A., Matsumoto, T., Kitano, Y. F., Nagai, S. & Yasuda, N. Discovery of the
875 northernmost habitat of the blue coral *Heliopora coerulea*: possible range expansion due to
876 climate change? *Galaxea J. Coral Reef Stud.* **19**, 1–2; 10.3755/galaxea.19.1_1 (2017).

877 14. Nakabayashi, A. *et al.* The potential role of temperate Japanese regions as refugia for the
878 coral *Acropora hyacinthus* in the face of climate change. *Sci. Rep.* **9**, 1892; 10.1038/s41598-
879 018-38333-5 (2019).

880 15. Yamano, H., Sugihara, K. & Nomura, K. Rapid poleward range expansion of tropical reef
881 corals in response to rising sea surface temperatures. *Geophys. Res. Lett.* **38**, L046474;
882 10.1029/2010GL046474 (2011).

883 16. Vargas-Ángel, B., Thomas, J. D. & Hoke, S. M. High-latitude *Acropora cervicornis*
884 thickets off Fort Lauderdale, Florida, USA. *Coral Reefs* **22**, 465–473; 10.1007/s00338-003-
885 0336-z (2003).

886 17. Serrano, E. *et al.* Rapid northward spread of a zooxanthellate coral enhanced by artificial
887 structures and sea warming in the western Mediterranean. *PLoS One* **8**, e52739;
888 10.1371/journal.pone.0052739 (2013).

889 18. Baird, A. H., Sommer, B. & Madin, J. S. Poleward range expansion of *Acropora* spp.

890 along the east coast of Australia. *Coral Reefs* **31**, 1063; 10.1007/s00338-012-0928-6 (2012).

891 19. Silverstein, R. N., Cunning, R. & Baker, A. C. Tenacious D: *Symbiodinium* in clade D
892 remain in reef corals at both high and low temperature extremes despite impairment. *J. Exp.*
893 *Biol.* **220**, 1192–1196; 10.1242/jeb.148239 (2017).

894 20. LaJeunesse, T. C. *et al.* Ecologically differentiated stress-tolerant endosymbionts in the
895 dinoflagellate genus *Symbiodinium* (Dinophyceae) Clade D are different species. *Phycologia*
896 **53**, 305–319; 10.2216/13-186.1 (2014).

897 21. Wicks, L. C., Sampayo, E., Gardner, J. P. A. & Davy, S. K. Local endemicity and high
898 diversity characterise high-latitude coral–Symbiodinium partnerships. *Coral Reefs* **29**, 989–
899 1003; 10.1007/s00338-010-0649-7 (2010).

900 22. Leydet, K. P. *et al.* Host-targeted RAD-Seq reveals genetic changes in the coral *Oculina*
901 *patagonica* associated with range expansion along the Spanish Mediterranean coast. *Mol.*
902 *Ecol.* **27**, 2529–2543; 10.1111/mec.14702 (2018).

903 23. Suzuki, G. & Fukami, H. Evidence of genetic and reproductive isolation between two
904 morphs of subtropical-dominant coral *Acropora solitaryensis* in the non-reef region of Japan.
905 *Zool. Sci.* **29**, 134–140; 10.2108/zsj.29.134 (2012).

906 24. Cumbo, V. R., Baird, A. H. & Van Oppen, M. J. H. The promiscuous larvae: flexibility in
907 the establishment of symbiosis in corals. *Coral Reefs* **32**, 111–120; 10.1007/s00338-012-
908 0951-7 (2013).

909 25. Pinsky, M. L., Selden, R. L. & Kitchel, Z. J. Climate-driven shifts in marine species
910 ranges: scaling from organisms to communities. *Annu. Rev. Mar. Sci.* **12**, 153–179;
911 10.1146/annurev-marine-010419-010916 (2020).

912 26. Hume, B. C. *et al.* Ancestral genetic diversity associated with the rapid spread of stress-

913 tolerant coral symbionts in response to Holocene climate change. *Proc. Natl. Acad. Sci. U. S.*
914 *A.* **113**, 4416–4421; 10.1073/pnas.1601910113 (2016).

915 27. Thornhill, D. J., Kemp, D. W., Bruns, B. U., Fitt, W. K. & Schmidt, G. W.
916 Correspondence between cold tolerance and temperate biogeography in a Western Atlantic
917 *Symbiodinium* (Dinophyta) lineage. *J. Phycol.* **44**, 1126–1135; 10.1111/j.1529-
918 8817.2008.00567.x (2008).

919 28. Baird, A. H., Guest, J. R. & Willis, B. L. Systematic and biogeographical patterns in the
920 reproductive biology of scleractinian corals. *Annu. Rev. Ecol. Evol. Syst.* **40**, 551–571;
921 10.1146/annurev.ecolsys.110308.120220 (2009).

922 29. Quigley, K. M., Willis, B. L. & Bay, L. K. Heritability of the *Symbiodinium* community in
923 vertically- and horizontally-transmitting broadcast spawning corals. *Sci. Rep.* **7**, 8219;
924 10.1038/s41598-017-08179-4 (2017).

925 30. Budd, A. F. & Pandolfi, J. M. Evolutionary novelty is concentrated at the edge of coral
926 species distributions. *Science* **328**, 1558–1561; 10.1126/science.1188947 (2010).

927 31. De Palmas, S. *et al. Symbiodinium* spp. associated with high-latitude scleractinian corals
928 from Jeju Island, South Korea. *Coral Reefs* **34**, 919–925; 10.1007/s00338-015-1286-y
929 (2015).

930 32. Ng, T. Y. & Ang, P. Low symbiont diversity as a potential adaptive strategy in a marginal
931 non-reefal environment: a case study of corals in Hong Kong. *Coral Reefs* **35**, 941–957;
932 10.1007/s00338-016-1458-4 (2016).

933 33. Reimer, J. D., Takishita, K. & Maruyama, T. Molecular identification of symbiotic
934 dinoflagellates (*Symbiodinium* spp.) from *Palythoa* spp. (Anthozoa: Hexacorallia) in Japan.
935 *Coral Reefs* **25**, 521–527; 10.1007/s00338-006-0151-4 (2006).

936 34. Abrego, D., Ulstrup, K. E., Willis, B. L. & van Oppen, M. J. Species–specific interactions
937 between algal endosymbionts and coral hosts define their bleaching response to heat and light
938 stress. *Proc. R. Soc. B Biol. Sci.* **275**, 2273–2282; 10.1098/rspb.2008.0180 (2008).

939 35. Ulstrup, K. E. & van Oppen, M. J. H. Geographic and habitat partitioning of genetically
940 distinct zooxanthellae (*Symbiodinium*) in *Acropora* corals on the Great Barrier Reef. *Mol.*
941 *Ecol.* **12**, 3477–3484; 10.1046/j.1365-294X.2003.01988.x (2003).

942 36. Lesica, P. & Allendorf, F. W. When are peripheral populations valuable for conservation?
943 *Conserv. Biol.* **9**, 753–760; 10.1046/j.1523-1739.1995.09040753.x (1995).

944 37. Coles, S. L. & Fadlallah, Y. H. Reef coral survival and mortality at low temperatures in
945 the Arabian Gulf: new species-specific lower temperature limits. *Coral Reefs* **9**, 231–237;
946 10.1007/BF00290427 (1991).

947 38. Crossland, C. J. Seasonal variations in the rates of calcification and productivity in the
948 coral *Acropora formosa* on a high-latitude reef. *Mar. Ecol. Prog. Ser.* **15**, 135–140;
949 10.3354/meps015135 (1984).

950 39. Denis, V. *et al.* Coverage, diversity, and functionality of a high-latitude coral community
951 (Tatsukushi, Shikoku Island, Japan). *PLoS One* **8**, e54330; 10.1371/journal.pone.0054330
952 (2013).

953 40. Yamano, H. & Namizaki, N. Corals on the front: changes of *Acropora solitaryensis*
954 colonies at Tateyama, Chiba Prefecture, Japan. *J. Jpn. Coral Reef Soc.* **11**, 71–72;
955 10.3755/jcrs.11.71 (2009).

956 41. Sugihara, K. et al. Zooxanthellate scleractinian corals of Tanegashima Island, Japan.
957 Center for Environmental Biology and Ecosystem Studies, National Institute for
958 Environmental Studies. Available at: https://www.nies.go.jp/biology/pdfs/pu_3.pdf

959 42. Chow, S. W. *et al.* A clear distinction and presence of *Acropora* aff. *divaricata* within
960 *Acropora* cf. *solitaryensis* species complex along their biogeographic distribution in East
961 Asia. *Sci. Rep.* **15**, 9739; 10.1038/s41598-025-90051-x (2025).

962 43. Nozawa, Y. & Okubo, N. Survival dynamics of reef coral larvae with special
963 consideration of larval size and the genus *Acropora*. *Biol. Bull.* **220**, 15–22;
964 10.1086/BBLv220n1p15 (2011).

965 44. Meeker, N. D., Hutchinson, S. A., Ho, L. & Trede, N. S. Method for isolation of PCR-
966 ready genomic DNA from zebrafish tissues. *Biotechniques* **43**, 610–614; 10.2144/000112619
967 (2007).

968 45. Richards, Z. T. *et al.* Integrated evidence reveals a new species in the ancient blue coral
969 genus *Heliopora* (Octocorallia). *Sci. Rep.* **8**, 15875; 10.1038/s41598-018-32969-z (2018).

970 46. Wu, Q. & Minamoto, T. Improvement of recovery yield of macro-organismal
971 environmental DNA from seawater samples. *Anal. Sci.* **39**, 713–720; 10.1007/s44211-023-
972 00280-1 (2023).

973 47. Miya, M. & Sado, T. DNA extraction from cartridge-type filters. In Environmental DNA
974 Survey and Experiment Manual Ver. 3.0 (eds Environmental DNA Society Environmental
975 DNA Technical Standardization Committee), 39–51 (2024). Available at:
976 https://ednasociety.org/wp-content/uploads/2024/08/環境 DNA 調査・実験マニュアル
977 _ver3_0.pdf

978 48. Suyama, Y. & Matsuki, Y. MIG-seq: an effective PCR-based method for genome-wide
979 single-nucleotide polymorphism genotyping using the next-generation sequencing platform.
980 *Sci. Rep.* **5**, 16963; 10.1038/srep16963 (2015).

981 49. Gordon, A. & Hannon, G. Fastx-toolkit: FASTQ/A short-reads pre-processing tools

982 (2010). Available at: http://hannonlab.cshl.edu/fastx_toolkit/index.html

983 50. Martin, M. Cutadapt removes adapter sequences from high-throughput sequencing reads.
984 *EMBnet J.* **17**, 10–12; 10.14806/ej.17.1.200 (2011).

985 51. Catchen, J. M., Amores, A., Hohenlohe, P., Cresko, W. & Postlethwait, J. H. Stacks:
986 building and genotyping loci de novo from short-read sequences. *G3* **1**, 171–182;
987 10.1534/g3.111.000240 (2011).

988 52. Rochette, N. C., Rivera-Colón, A. G. & Catchen, J. M. Stacks 2: Analytical methods for
989 paired-end sequencing improve RADseq-based population genomics. *Mol. Ecol.* **28**, 4737–
990 4754; 10.1111/mec.15253 (2019).

991 53. Shinzato, C. *et al.* Using the *Acropora digitifera* genome to understand coral responses to
992 environmental change. *Nature* **476**, 320–323; 10.1038/nature10249 (2011).

993 54. Shoguchi, E. *et al.* Two divergent *Symbiodinium* genomes reveal conservation of a gene
994 cluster for sunscreen biosynthesis and recently lost genes. *BMC Genomics* **19**, 1–11;
995 10.1186/s12864-018-4857-9 (2018).

996 55. Li, H. & Durbin, R. Fast and accurate short read alignment with Burrows–Wheeler
997 transform. *Bioinformatics* **25**, 1754–1760; 10.1093/bioinformatics/btp324 (2009).

998 56. Foll, M. & Gaggiotti, O. A genome-scan method to identify selected loci appropriate for
999 both dominant and codominant markers: a Bayesian perspective. *Genetics* **180**, 977–993;
1000 10.1534/genetics.108.092221 (2008).

1001 57. Lischer, H. E. & Excoffier, L. PGDSpider: an automated data conversion tool for
1002 connecting population genetics and genomics programs. *Bioinformatics* **28**, 298–299;
1003 10.1093/bioinformatics/btr642 (2012).

1004 58. Peakall, R. & Smouse, P. E. GenAlEx 6.5: genetic analysis in Excel. Population genetic

1005 software for teaching and research—an update. *Bioinformatics* **28**, 2537–2539;
1006 10.1093/bioinformatics/bts460 (2012).

1007 59. Pritchard, J. K., Wen, X. & Falush, D. Documentation for STRUCTURE software:
1008 Version 2.3. University of Chicago, Chicago, IL (2010). Available at:
1009 https://pic.biodiscover.com/files/c/9p/biodiscover1385456414.7278405.pdf

1010 60. Evanno, G., Regnaut, S. & Goudet, J. Detecting the number of clusters of individuals
1011 using the software STRUCTURE: a simulation study. *Mol. Ecol.* **14**, 2611–2620;
1012 10.1111/j.1365-294X.2005.02553.x (2005).

1013 61. Earl, D. A. & vonHoldt, B. M. STRUCTURE HARVESTER: a website and program for
1014 visualizing STRUCTURE output and implementing the Evanno method. *Conserv. Genet.*
1015 *Resour.* **4**, 359–361; 10.1007/s12686-011-9548-7 (2012).

1016 62. Kopelman, N. M., Mayzel, J., Jakobsson, M., Rosenberg, N. A. & Mayrose, I. Clumpak: a
1017 program for identifying clustering modes and packaging population structure inferences
1018 across K. *Mol. Ecol. Resour.* **15**, 1179–1191; 10.1111/1755-0998.12387 (2015).

1019 63. Jombart, T. adegenet: an R package for the multivariate analysis of genetic markers.
1020 *Bioinformatics* **24**, 1403–1405; 10.1093/bioinformatics/btn129 (2008).

1021 64. Jombart, T. & Ahmed, I. adegenet 1.3–1: new tools for the analysis of genome-wide SNP
1022 data. *Bioinformatics* **27**, 3070–3071; 10.1093/bioinformatics/btr521 (2011).

1023 65. Jombart, T., Devillard, S. & Balloux, F. Discriminant analysis of principal components: a
1024 new method for the analysis of genetically structured populations. *BMC Genet.* **11**, 94;
1025 10.1186/1471-2156-11-94 (2010).

1026 66. LaJeunesse, T. C. Diversity and community structure of symbiotic dinoflagellates from
1027 Caribbean coral reefs. *Mar. Biol.* **141**, 387–400; 10.1007/s00227-002-0829-2 (2002).

1028 67. Coleman, A. W., Suarez, A. & Goff, L. J. Molecular delineation of species and syngens in
1029 volvocacean green algae (Chlorophyta). *J. Phycol.* **30**, 80–90; 10.1111/j.0022-
1030 3646.1994.00080.x (1994).

1031 68. Hall, T. A. BioEdit: a user-friendly biological sequence alignment editor and analysis
1032 program for Windows 95/98/NT. Nucl. Acids Symp. Ser. 41, 95–98 (1999).

1033 69. Librado, P. & Rozas, J. DnaSP v5: a software for comprehensive analysis of DNA
1034 polymorphism data. *Bioinformatics* **25**, 1451–1452; 10.1093/bioinformatics/btp187 (2009).

1035 70. Bandelt, H. J., Forster, P. & Röhl, A. Median-joining networks for inferring intraspecific
1036 phylogenies. *Mol. Biol. Evol.* **16**, 37–48; 10.1093/oxfordjournals.molbev.a026036 (1999).

1037 71. Hume, B. C. *et al. Symbiodinium thermophilum* sp. nov., a thermotolerant symbiotic alga
1038 prevalent in corals of the world's hottest sea, the Persian/Arabian Gulf. *Sci. Rep.* **5**,
1039 8562;10.1038/srep08562 (2015).

1040 72. Hume, B. C. *et al.* Corals from the Persian/Arabian Gulf as models for thermotolerant
1041 reef-builders: prevalence of clade C3 *Symbiodinium*, host fluorescence and ex situ
1042 temperature tolerance. *Mar. Pollut. Bull.* **72**, 313–322; 10.1016/j.marpolbul.2012.11.032
1043 (2013).

1044 73. Nagai, S. *et al.* Comparing PCR-generated artifacts of different polymerases for improved
1045 accuracy of DNA metabarcoding. *Metabarcoding Metagenomics* **6**, e77704;
1046 10.3897/mbmg.6.77704 (2022).

1047 74. Hume, B. C. *et al.* SymPortal: a novel analytical framework and platform for coral algal
1048 symbiont next-generation sequencing ITS2 profiling. *Mol. Ecol. Resour.* **19**, 1063–1080;
1049 10.1111/1755-0998.13004 (2019).

1050 75. Eren, A. M. *et al.* Minimum entropy decomposition: unsupervised oligotyping for

sensitive partitioning of high-throughput marker gene sequences. *ISME J.* **9**, 968–979; 10.1038/ismej.2014.195 (2015).

76. Brooks, M. E. *et al.* glmmTMB balances speed and flexibility among packages for zero-inflated generalized linear mixed modeling. *R J.* **9**, 378–400; https://digitalcommons.unl.edu/cgi/viewcontent.cgi?article=1637&context=r-journal (2017).

77. Lüdecke, D., Ben-Shachar, M. S., Patil, I., Waggoner, P. & Makowski, D. performance: an R package for assessment, comparison and testing of statistical models. *J. Open Source Softw.* **6**, 3139; 10.21105/joss.03139 (2021).

Acknowledgements

We are also grateful to Ms. E. Nagahiro, Ms. R. Kubota and Ms. M. Nishijima for their assistance with the experiments, and Y. Fujino, M. Murakami, H. Hotoku, K. Nomura and T. Mezaki for their assistance with the sampling. Computations were partially performed on the NIG supercomputer at the ROIS National Institute of Genetics. This work was supported by JST, CREST, JPMJCR23J2, JSPS KAKENHI Grant Number 23H00529, 22KJ1108, and the Environment Research and Technology Development Fund (4RF-1501 and 4-1304) of the Ministry of the Environment, Japan, and Daiichi Sankyo Foundation of Life Science. We used generative AI tools such as ChatGPT and DeepL for grammar revision and text improvement to polish the research paper written by non-native authors.

Contributions

Conceptualization, N. Y.; Experiment, A. S., M. K., H. T. and K. T.; Analysis, A. S., M. K., K. T., T. N., A. I., T. Y., S. N., T. K., H. Y. and K. G.; Sampling and Investigation, A. S., K.

T., S. S., Y. K., H.F. and N. Y.; Writing – review & editing, M. K. and N. Y. All authors approved the final manuscript.

Ethics declarations

Field sampling was conducted under the permits and notifications described in the Methods, with prior agreement from relevant local fisheries cooperatives where required. Coral sampling was performed in accordance with local regulations and with efforts to minimize damage to colonies.

Competing interests

The authors declare no competing interests.

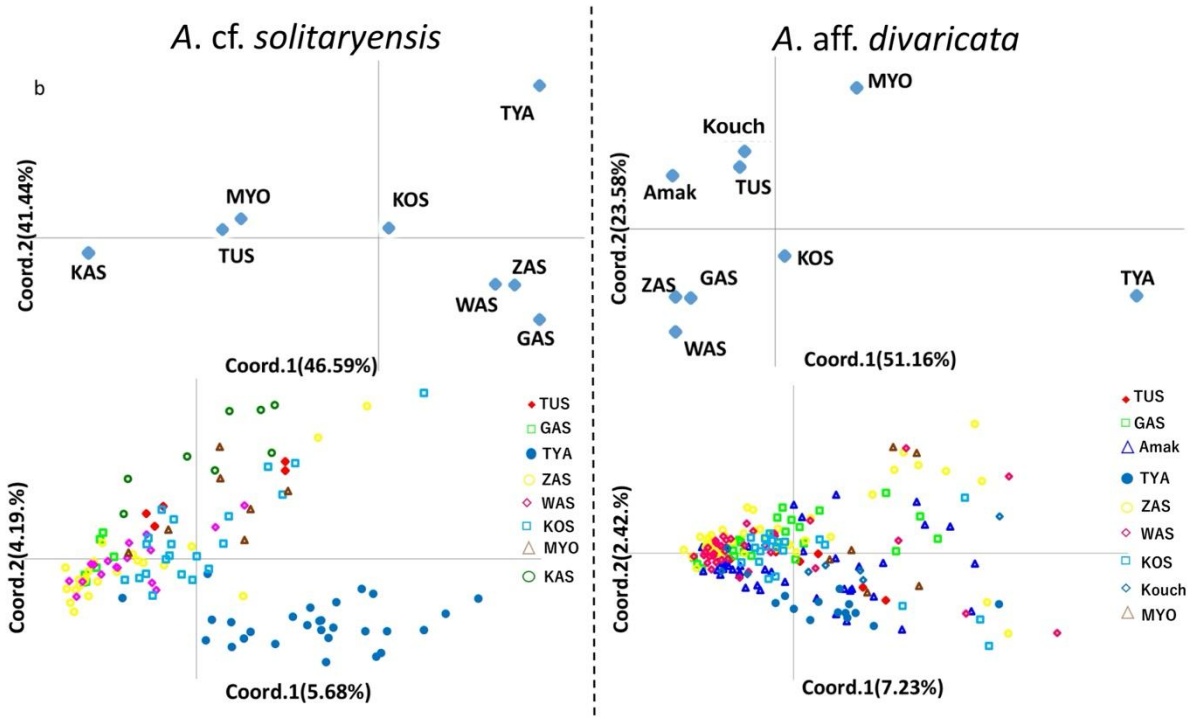
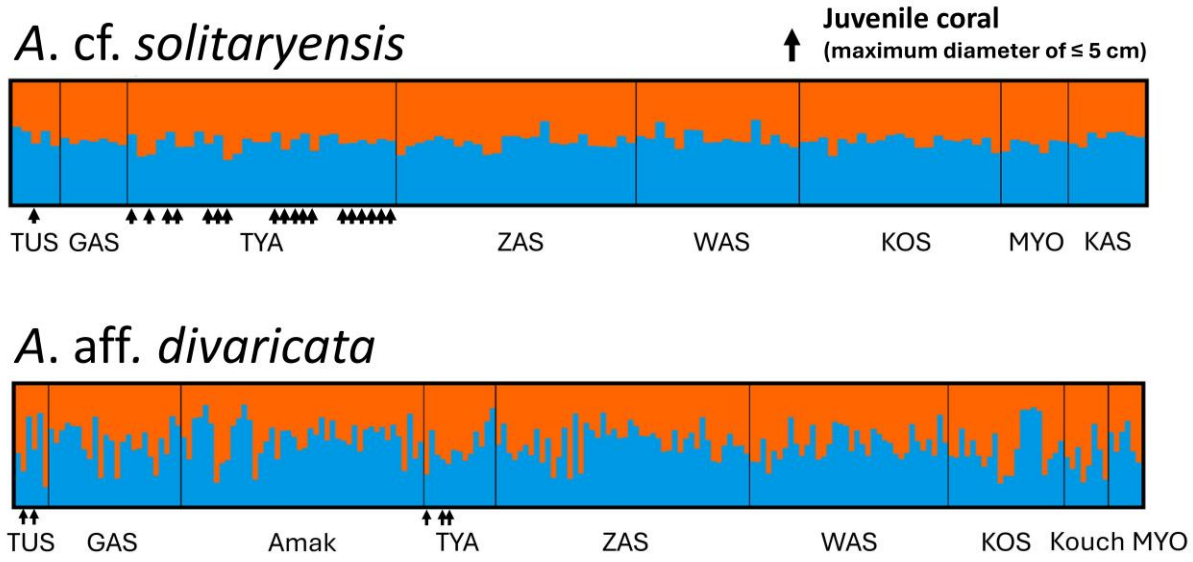


Fig. 1 PCoA results for the host coral species *A.* cf. *solitaryensis* (left) and *A.* aff. *divaricata* (right), shown using population-based data (top) and individual-based data (bottom).



1087

1088

1089 **Fig. 2 STRUCTURE bar plots for the two coral species.** Each individual's genetic

1090 membership is estimated across the inferred ancestral clusters, represented by different

1091 colors. The x-axis represents individual corals, and the y-axis represents the proportional

1092 assignment to the two inferred ancestral clusters ($K = 2$).

1093

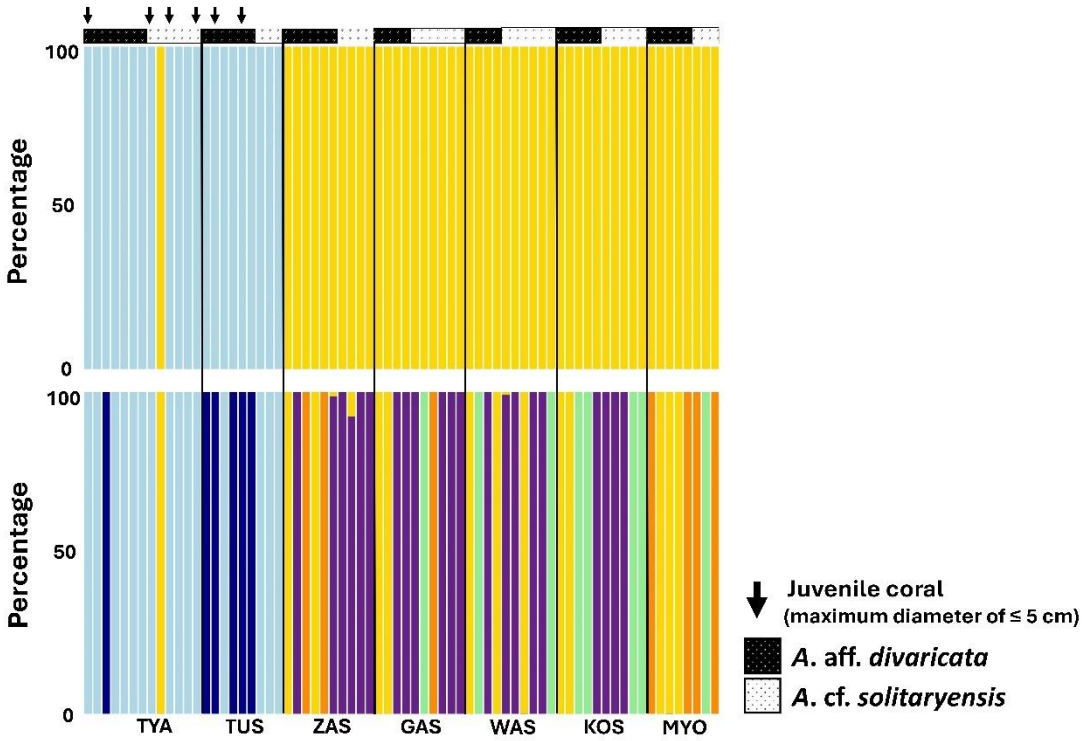
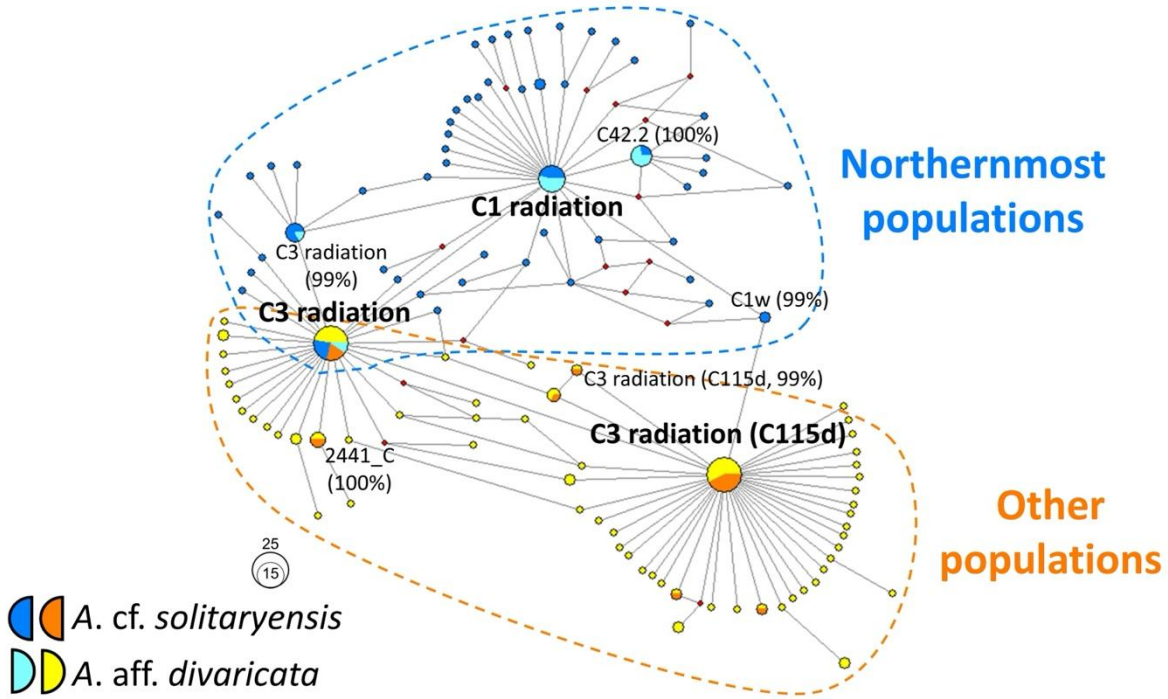


Fig. 3 DAPC bar plots based on genome-wide SNP data from algal symbionts in two coral species (*A.* cf. *solitaryensis* and *A.* aff. *divaricata*). The top hatch bar indicates the coral species (black–white hatch = *A.* aff. *divaricata*, white–black hatch = *A.* cf. *solitaryensis*). The upper panel shows membership probabilities for $K = 2$, corresponding to the ΔK optimum from STRUCTURE, and the lower panel shows membership probabilities for $K = 6$, corresponding to the BIC optimum from DAPC. Each vertical bar along the x-axis represents an individual sample, while the y-axis indicates the proportional membership of that individual in each SNP-based cluster. Different colors represent distinct genetic clusters identified by the DAPC analysis. Notably, the symbiont composition in marginal areas (TYA: Tateyama, TUS: Tsushima) differs markedly from that in the other temperate regions.



1106

1107 **Fig. 4 The haplotype network of *Cladocopium* spp. sequences from the two host coral**
1108 **species based on ITS2 sequences.** The *Cladocopium* spp. haplotypes within the blue and
1109 light-blue are from the northernmost populations (Tateyama and Tsushima), while those
1110 within the orange and yellow dot are from other areas. This network includes juvenile
1111 samples. By contrast, juveniles were excluded from the adult-only SymPortal visualization
1112 shown in Fig. 5.

1113

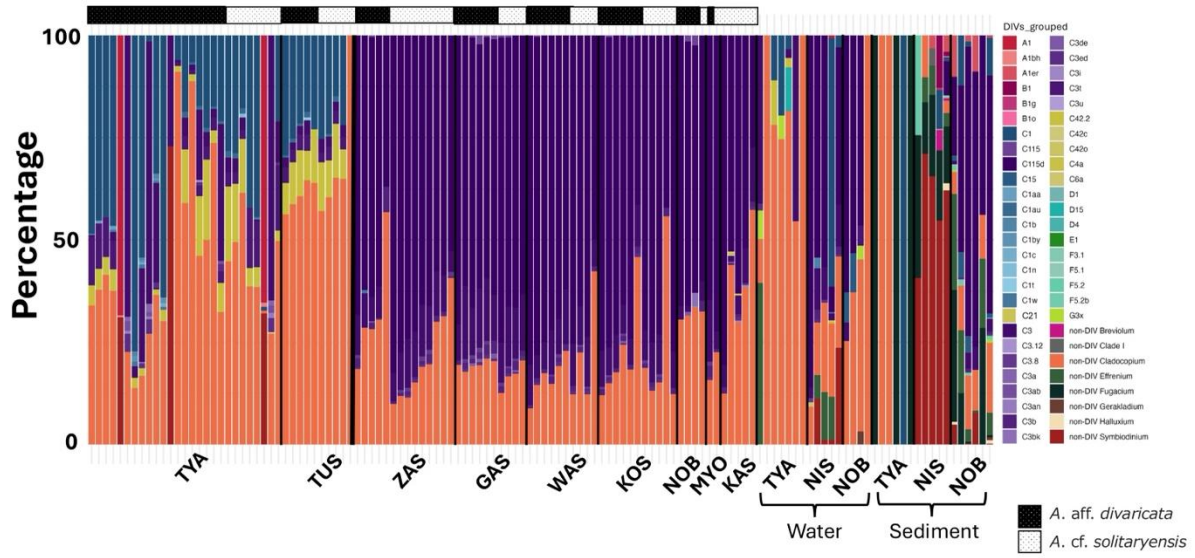


Fig. 5 Symbiodiniaceae ITS2 metabarcoding profiles from adult corals, seawater, and sediments. Only libraries amplified with SYM_VAR_5.8S2/SYM_VAR_REV are shown. This figure includes only adult coral samples. Libraries were processed in SymPortal to infer ITS2 type profiles (sets of recurrent, co-occurring DIVs). Each vertical bar represents one sample; for coral samples, the header hatch indicates host species (black–white hatch = *A.* aff. *divaricata*, white–black hatch = *A.* cf. *solitaryensis*). Environmental seawater and sediment samples are shown at the far right. Stacks show the relative read abundance of C1-radiation and C3-radiation ITS2 profiles, the latter including profiles containing the DIV C115d; minor *Cladocopium* types outside C1/C3 and profiles from other Symbiodiniaceae genera (e.g., Symbiodinium [A-type], Fugacium [F-type], Gerakladium [G-type]) are shown separately.

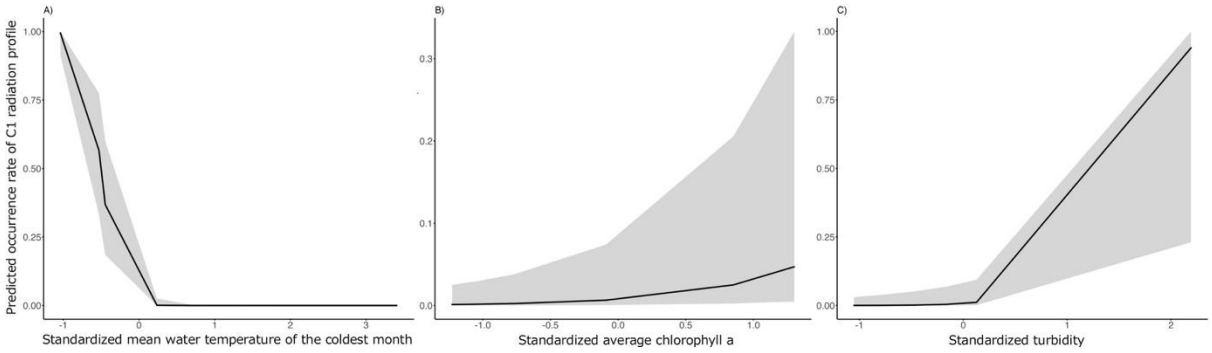
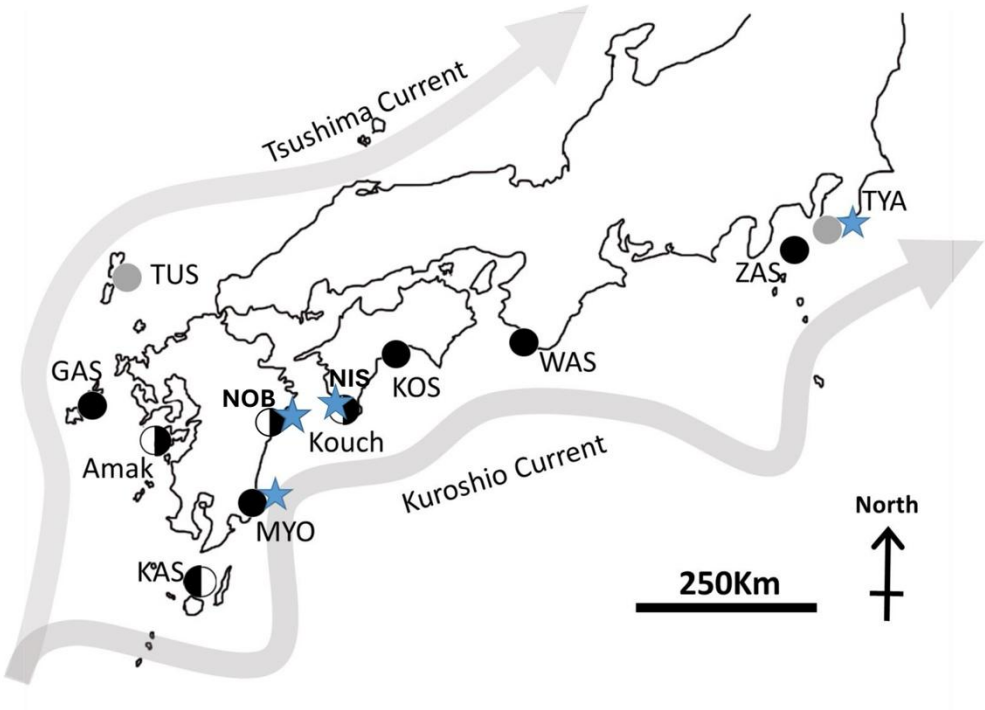


Fig. 6 Site-level GLMM-predicted occurrence probability of C1-radiation profiles across environmental gradients. Solid lines show mean predicted probabilities from the best-supported GLMM, and shaded ribbons indicate model-based 95% confidence intervals. Because environmental predictors were measured at the site level, these curves represent exploratory site-level associations rather than independent colony-level causal effects. (A) Predicted occurrence declines with increasing standardized mean seawater temperature of the coldest month. (B) Predicted occurrence increases with increasing standardized mean chlorophyll a concentration. (C) Predicted occurrence increases with increasing standardized turbidity.



1137

1138 **Fig. 7 Sampling sites of *A*. aff. *divaricata* (filled on the right side in white), *A*. cf.**

1139 ***solitaryensis* (filled on the left side in black), and environmental samples (star) in this**

1140 **study.** The northernmost habitats are shown in gray. The site abbreviations are as follows;

1141 KAS: Tanegashima, Amak: Amakusa, GAS: Goto, MYO: Miyazaki, NOB: Nobeoka, TUS:

1142 Tsushima, Kouch: Tatsukushi, NIS: Nishidomari, KOS: Yokonami, WAS: Wakayama, ZAS:

1143 Shikinejima, TYA: Tateyama.

1144

1145 **Table 1: Samples used in this study. * indicates the northernmost habitats in both coral**

1146 **species (*A.* cf. *solitaryensis* (AcS) and *A.* aff. *divaricata* (AaD)).**

Table 1: Samples used in this study. * indicates the northernmost habitats in both coral species (*A. cf. solitaryensis* (AcS) and *A. aff. divaricata* (AaD)).

	Coral sampling locations	Coordinate	Sampling date	Coral genetic structure (MIGseq 16 primers)		Symbiotic algal genome DAPC (MIGseq 8 primers)		ITS2 subcloning (ITSintfor2/ITS-Reverse)		Symportal (ITSintfor2/ITS-Reverse)		Symportal (SYM_VAR_5.8S2/SYM_VAR_REV)	
				AcS	AaD	AcS	AaD	AcS	AaD	AcS	AaD	AcS	AaD
Kuroshio current	Tateyama*	34° 59'27.00"N, 139° 49'4.00"E	Oct. 2018, Jul. and Sep. 2024	28(18)	13(2)	6(3)	7(1)	9	8	3	2	8	19
	Shikinejima	34° 19'00.04"N, 139° 12'36.35"E	Sep. 2016	25	46	4	6	3	4	5	5	9	5
	Wakayama	33° 28'24.83"N, 135° 45'48.01"E	Jun. and Jul. 2016	17	36	6	4	1	4	2	2	4	6
	Yokonami	33° 24'09.72"N, 133° 24'29.48"E	May. 2017	21	21	5	5	1	1	7	6	5	6
	Tatsukushi	32° 45'49.33"N, 132° 51'38.39"E	Oct. 2011	0	8	0	0	0	0	0	0	0	0
	Miyazaki	31° 31'3.42"N, 131° 24'40.44"E	Dec. 2017	7	6	3	5	3	1	1	1	1	1
	Nobeoka	32° 39'44.4"N, 131° 48'40.60"E	Feb. 2026	–	–	–	–	–	–	–	–	1	3
	Tanegashima	30° 35'54.68"N, 130° 59'28.44"E	Aug. 2018	8	0	0	0	3	0	0	0	5	0
Tsushima current	Tsushima*	34° 25'25.00"N, 129° 16'0.00"E	Nov. 2017	5(1)	6(2)	3	6(2)	2	2	4	1	5	5
	Goto	32° 34'21.08"N, 128° 53'48.73"E	Nov. 2016	7	24	6	4	3	3	1	6	4	6
	Amakusa	32° 33'16.16"N, 129° 59'59.91"E	Sep. 2009	0	44	0	0	0	0	0	0	0	0
Sea water sample	Tateyama	34° 59'27.00"N, 139° 49'4.00"E	Oct. 2020, Feb. 2025	-		-		61		-		7	
	Nishidomari	32° 46'40.26"N, 132° 43'55.80"E	Jan. 2026					-				5	
	Nobeoka	32° 39'44.4"N, 131° 48'40.60"E	Feb. 2026					-				4	
	Miyazaki	31° 38'70.688" N, 131° 30'92.523" E	Mar. 2020					27				0	
Sediment sample	Tateyama	34° 59'27.00"N, 139° 49'4.00"E	Feb. 2025	-		-		-		-		6	
	Nishidomari	32° 46'40.26"N, 132° 43'55.80"E	Jan. 2026									5	
	Nobeoka	32° 39'44.4"N, 131° 48'40.60"E	Feb. 2026									6	

※The number in parentheses indicates the number of juvenile corals with a maximum diameter ≤5 cm.

Supplementary Files

This is a list of supplementary files associated with this preprint. Click to download.

- DescriptionofadditionalsupplementaryfilesCommsBio.docx
- XXXSupplementaryData18260718.xlsx
- XXXSupplementaryInformation260718.docx